UNIVERSITAT POLITÈCNICA DE VALÈNCIA

UNIVERSITAT POLITÈCNICA DE VALÈNCIA

ESCOLA TÈCNICA SUPERIOR D'ENGINYERIA AGRONÒMICA I DEL MEDI NATURAL

Escola Tècnica Superior d'Enginyeria Agronòmica i del Medi Natural

BACHELOR'S DEGREE IN BIOTECHNOLOGY

Academic year 2018-219

EFFECT OF A FASUDIL NANOCONJUGATE AND TRANSPLANTATION OF NEURAL PRECURSORS ON NEURAL REGENERATION IN A SPINAL CORD INJURY CHRONIC MODEL.

ROLE OF AMPK SIGNALING IN THE EFFECT OF FASUDIL OVER NEURITE GROWTH AND DIFFERENTIATION IN NEURAL PRECURSORS.

AUTHOR: DON EDUARDO FERNÁNDEZ ORTUÑO

ACADEMIC TUTOR: PROF. DR. ESTHER GIRALDO REBOLOSO

EXTERNAL CO-TUTOR: DR. VICTORIA MORENO MANZANO

VALENCIA, JULY 2019

TITLE:

Effect of a Fasudil nanoconjugate and transplantation of neural precursors on neural regeneration in a spinal cord injury chronic model. Role of AMPK signaling in the effect of Fasudil over neurite growth and differentiation in neural precursors.

ABSTRACT:

Despite the regenerative potential of neural precursors and the axonal and synaptic remodeling capacity, it has not been possible to find effective means of cure for spinal cord injury (SCI) and it remains as one of the traumatisms having most drastic consequences for the quality of life of those being affected. Several approaches are under development in order to manipulate the lesion microenvironment. At this regard, cell therapy with ependymal neural precursors is considered as one of the spearheading strategies for the consecution of an effective treatment for SCI. Transfer of neural precursors epSPCs (ependymal stem/progenitor cells) into the injured tissue aims at two objectives: a modification of the microenvironment, which could either boost the process of tissue regeneration or limit its barriers; as well as their integration in the nervous tissue, which is expected to strengthen the functional recuperation.

Additionally, after a SCI, synaptic remodeling and axonal circuit reorganization could be implemented via the modification of inhibitory signaling pathways or increasing the intrinsic growing potential of neurons. Inhibition of the Rho/ROCK signaling pathway is one of the molecular mechanisms known to stimulate neural growth. In this sense, Fasudil is a compound that inhibits this pathway and its application has been related with neural regeneration. So as to attain a longer action of this drug, it has been conjugated with a polyglutamate polymer, which confers it a higher stability in the tissue, allowing a more distended and continuous release for a more extended time, which is expected to elicit a better response for the regeneration of the tissue.

Taking this into consideration, a combinatory therapy involving neural precursors and Fasudil could have a synergic effect on the recuperation of the injured tissue in the spinal cord. Along the present project, the effect of different treatments combining these factors are analyzed in a rat chronic model of SCI.

Notwithstanding, Fasudil neuroprotective and neuroregenerative effects have not been completely characterized and there could be other signaling pathways being implied. The cell energetic balance regulator AMPK has been associated with neuroprotection and axonal growth. As such, in order to elucidate a possible interaction between Fasudil and this pathway, the effects of several treatments comprising Fasudil, an AMPK activator (metformin) and an AMPK inhibitor (compound C) on neurite growth and differentiation of epSPCs are studied as well.

KEY WORDS:

AMPK, epSPCs, fasudil, metformin, neural progenitors, neural regeneration, Rho/ROCK, spinal cord injury.

TÍTULO

Efecto de un nanoconjugado de Fasudil y del trasplante de precursores neurales sobre la regeneración neuronal en un modelo crónico de lesión medular. Papel de la señalización de AMPK sobre el efecto del Fasudil en el crecimiento de neuritas y diferenciación en precursores neurales.

RESUMEN

A pesar del potencial regenerativo de precursores neurales y de la capacidad de remodelación axonal y sináptica, la lesión medular (LM) se mantiene sin cura y como uno de los traumatismos con consecuencias más drásticas para la calidad de vida de los afectados. Distintas estrategias se están desarrollando para modular el microambiente de la lesión. En este punto, la terapia celular con precursores neurales ependimarios se ha consolidado como una de las puntas de lanza en la consecución de una terapia efectiva para la LM. El trasplante de precursores neurales epSPCs (ependymal stem/progenitor cells) en el tejido lesionado se realiza con dos objetivos: que induzcan una modificación del microambiente que reduzca las barreras a la regeneración o que la promueva, así como que logren integrarse y formar parte del tejido nervioso, fortaleciendo la recuperación funcional.

Por otro lado, después de una LM, la remodelización sináptica y la reorganización del circuito axonal puede ser implementada mediante la modulación de señalización inhibitoria o aumentando el potencial de crecimiento intrínseco de las neuronas. Uno de los mecanismos moleculares para la estimulación del crecimiento neuronal asentados es la inhibición de la vía de señalización Rho/ROCK. El compuesto Fasudil inhibe esta vía y su aplicación ya ha sido relacionada con la regeneración neuronal en este sentido. Para una mejor acción prolongada del fármaco, este ha sido conjugado con un polímero de poliglutamato que le proporciona una mayor estabilidad en el tejido, permitiendo una liberación continuada durante un mayor tiempo, lo que se espera que tenga un mejor efecto en la regeneración tisular.

Teniendo esto en cuenta, una terapia combinatoria con precursores neurales y Fasudil podría tener un efecto sinérgico sobre la recuperación del tejido lesionado en la médula. En este trabajo se analiza en un modelo de LM crónico en rata el efecto de distintos tratamientos que combinan estos factores.

No obstante, los efectos neuroprotectores y neurorregeneradores del Fasudil no han sido completamente caracterizados y podría haber otras vías de señalización implicadas. En este ámbito, el regulador del balance energético celular AMPK ha sido relacionado con neuroprotección y crecimiento axonal. Por ello, para tratar de dilucidar una posible interacción del Fasudil en esta vía, también se estudian los efectos sobre el crecimiento de neuritas y la diferenciación en epSPCs sometidas a tratamientos con Fasudil, con un activador de AMPK (metformina) y con un inhibidor (el compuesto C).

PALABRAS CLAVE:

AMPK, epSPCs, Fasudil, lesión medular, metformina, progenitores neurales, regeneración neuronal, Rho/ROCK.

TÍTOL:

Efecte d'un nanoconjugat de Fasudil i del trasplantament de precursors neurals sobre la regeneració neuronal en un model crònic de lesió medul·lar. Paper de la senyalització de AMPK en l'efecte del Fasudil sobre el creixement de neurites i diferenciació en precursors neurals.

RESUM:

Malgrat el potencial regeneratiu de precursors neurals i de la capacitat de remodelació axonal, la lesió medul·lar (LM) es manté sense cap cura i com un dels traumatismes amb conseqüències més dramàtiques per a la qualitat de vida dels afectats. Diverses estratègies estan en desenvolupament per modular el microambient de la lesió. En aquest punt, la teràpia cel·lular amb precursors neurals ependimaris s'ha consolidat com una de les principals avantguardes en la consecució d'una teràpia cel·lular efectiva per a la LM. El trasplantament de precursors neurals epSPCs (ependymal stem/progenitor cells) en el teixit afectat es realitza amb dos objectius: que induïsquen una modificació al microambient que reduïsca les barreres a la regeneració o que la promoga, així com aconseguir la seua integració i formar part del teixit nerviós, enfortint la recuperació funcional.

D'altra banda, després d'una LM, la remodelació sinàptica i la reorganització del circuit axonal pot ser implementada mitjançant la modulació de senyalització inhibitòria o augmentant el potencial de creixement intrínsec de les neurones. Un dels mecanismes moleculars establerts per a l'estimulació del creixement neuronal és la inhibició de la via de senyalització Rho/ROCK. El compost Fasudil inhibeix aquesta via i la seua aplicació ja ha sigut relacionada amb la regeneració neuronal en aquest sentit. Per a una millor acció prolongada del fàrmac, aquest ha sigut conjugat amb un polímer de poli-glutamat que li proporciona una major estabilitat en el teixit, permetent un alliberament continuat durant un major temps, la qual cosa s'espera que tinga un millor efecte en la regeneració tissular.

Tenint això en compte, una teràpia combinatòria amb precursors neurals i Fasudil podria tindre un efecte sinèrgic sobre la recuperació del teixit lesionat en la medul·la. En aquest treball s'analitza en un model de LM crònic en rata l'efecte de diferents tractaments que combinen aquests factors.

No obstant això, els efectes neuroprotectors i neurorregeneradors del Fasudil no han sigut completament caracteritzats i podria haver-hi altres vies de senyalització implicades. En aquest àmbit, el regulador del balanç energètic cel·lular AMPK ha sigut relacionat amb neuroprotecció i creixement axonal. Per això, per a tractar de dilucidar una possible interacció del Fasudil en aquesta via, també s'estudien els efectes sobre el creixement de neurites i la diferenciació en epSPCs sotmeses a tractaments amb Fasudil, amb un activador d'AMPK (metformina) i amb un inhibidor (compost C).

Paraules clau:

AMPK, epSPCs, lesió medul·lar, Fasudil, metformina, progenitors neurales, regeneració neuronal, Rho/ROCK.

Author

Don Eduardo Fernández Ortuño

Academic Tutor

Prof. Dr. Esther Giraldo Reboloso

External Co-tutor

Dr. Victoria Moreno Manzano

Location and date

Valencia, July 2019

APPRECIATIONS

I am not a person who likes talking about what is obvious, but here some words must be said.

I thank Dr. Victoria Moreno Manzano for accepting me in her research group. I also express my gratitude to the whole research group for their help, closeness and joy. Specially, I must thank my tutor, Esther, for her patience and her commitment with the students; Mara, for her assistance and cheerful humor, despite the long hours she works; and Marina, for her good practical piece of advice and rules of thumb.

But my highest gratitude goes to my parents. Now I realize how much effort they put in our education, mine and my sister's, and I must say clearly that I certainly would not have been successful in my academic life so far without them being an example of how sacrifices pay off. I thank my father, Francis, for he taught me that things must be done properly. I thank my mother, Carina, for she taught me that one must fight for the thins they want.

No soy alguien a quien le guste decir las cosas que son obvias, pero aquí se hace necesario.

Agradezco a la Dra. Victoria Moreno Manzano que me permitiera ser parte de su grupo, y agradezco a todo el grupo su ayuda, su cercanía y su ánimo alegre. En especial, debo darle las gracias a mi tutora, por su paciencia y su compromiso con sus alumnos; a Mara, por su buen humor y su jovialidad, a pesar de las muchas horas de trabajo; y a Marina, por sus consejos y trucos.

Pero mi mayor gratitud es hacia mis padres. Ahora cuando uno crece se da cuenta del esfuerzo que pusieron en la educación mía y de mi hermana, Carolina, y debo decir claramente que no habría tenido el éxito académico sin ellos como ejemplo de que los sacrificios y el esfuerzo merecen la pena. Le doy las gracias a mi padre, Francis, por enseñarme a que las cosas se hacen bien. Le doy las gracias a mi madre, Carina, por enseñarme que hay que luchar por las cosas.

ABBREVIATIONS AND ACRONYMS.

AMPK:	AMP-activated protein kinase
BSA:	Bovine Serum Albumin
BSPB:	Blood-Spinal Cord Barrier
CaM:	Calmodulin
CC:	Compound C.
ChABC:	Chondroitinase ABC
CNS:	Central Nervous System
CREB1:	cAMP-responsive element binding protein 1
CSPGs:	Chondroitin Sulfate Proteoglycans
DLK:	Dual Leucine Zipper-Bearing Kinase
ECM:	Extra Cellular Matrix
EDTA:	Ethylenediaminetetraacetic acid
EGF:	Epidermal Growth Factor
epSPCs:	ependymal Stem Progenitor Cells
ERKS:	Extracellular Signal Related Kinases
Fas50:	Fasudil at 50 µmolar
Fas100:	Fasudil at 100 µmolar
FF:	Free Fasudil
FGF:	Fibroblast Growth Factor
GAP43:	Growth Associated Protein 43
GFAP:	Glial Fibrillary Acid Protein
GFP:	Green Fluorescent Protein.
HATs:	Histone Acetyl Transferases
HDACs:	Histone Deacetylases
HE:	Hematoxylin-Eosin
HT:	Healthy Tissue
ICQ:	Immunocytochemistry
IHQ:	Immunohistochemistry
iNOS:	Inducible nitric oxide synthase
JNK:	JUN-N terminal kinase
LC:	Lesion Core
LPA:	Lisophosphatidic acid
MAG:	Myelin Associated Glycoprotein
MAPCs:	Multipotent Adult Progenitor Cells
Met:	Metformin7
mTOR:	Mammalian Target or Rapamycin
MSCs:	Mesenchymal Stem Cells
MN:	Motor Neuron
NAC:	N-acetylcysteine
NGS:	Normal Goat Serum

NSC:	Neural Stem Cell
NSPCs:	Neural Stem Progenitor Cells
OECs:	Olfactory Ensheathing Cells
OMgp:	Oligodendrocyte-Myelin glycoprotein
OPCS:	Oligodendrocyte Progenitor Cells
PGA:	Polyglutamic acid
PKC:	Protein Kinase C
PLP:	Perilesion Perimeter
PTEN:	Phosphatase and Tensin homologue
PVDF:	Polyvinylidene fluoride
RGM:	Repulsive Guidance Molecule
ROS:	Reactive Oxygen Species
SCI:	Spinal Cord Injury
STAT3:	Signal Transducer and Activator Of Transcription 3
SOCS3:	Suppressor Of Cytokine Signaling 3
SSFas:	conjugated fasudil
SSFas50:	conjugated fasudil at 50 µmolar,
SSFas100:	conjugated fasudil at 100 µmolar
TBST:	Tris Buffered Saline- Tween
TGF-β:	Transforming Growth Factor β
TF:	Transcription Factor
WB:	Western Blot.
WHO:	World Health Organization

TABLES AND FIGURES.

Tables.

Figures

TABLA DE CONTENIDO

I. INTRODUCTION

Spinal cord injury (SCI) refers to any damage on the spinal cord leading to motor, sensory and autonomic impairment, this having devastating consequences for the affected person at self-health and social dimensions. Even if pathologies other than traumatic can produce SCI (tumors, degenerative diseases, vascular and autoimmune disorders) (Grassner et al., 2016), traumatisms constitute indeed the main cause (Lee et al., 2014). Apart from the nervous system related affections, there are often secondary complications, including muscular atrophy, respiratory disorders (e.g. pneumonia, pulmonary edema), vascular disorders (e.g., deep venous thrombosis), post-injury/surgery, urinary and respiratory infections, pressure sores and bone demineralization, among others (Sezer, Akkuş, & Uğurlu, 2015, Hagen, 2015). Importantly, SCI-affected patients are 2 to 5 times more likely to have a premature death (WHO, 2013). Taking into account that most of the new 250000-500000 cases per year appear at young ages (20-29 years for males and 15-19 years for females) (WHO, 2013) and the daunting horizon for the person affected, development of an effective therapy for SCI is one of the holy grails of regenerative medicine.

I. II CHARACTERIZATION OF THE SPINAL CORD INJURY.

Structure of the lesion.

As described by Sofroniew (2018), the SCI can be structured into three histologically different entities (**Fig. 1**). The **non-neural lesion core** is the epicenter of the lesion and is conformed by an unorganized stromal compartment, composed by the remnants of cell debris, remaining macrophages and other injury-associated cells, such as fibroblasts, pericytes and fibrocytes (Burda & Sofroniew 2014), and extracellular matrix (ECM) molecules, e.g., fibronectins, collagens, proteoglycans and laminins, which can have a crucial role in axonal guidance or repelling for circuit remodeling and growth. In any case, the lesion core will be no source of regeneration and presents molecular impediments to axon regeneration (Hermanns et al., 2006), although modification of this toxic environment can be envisaged so as to allow axonal growth across it. The non-neural lesion core is delimited by a surrounding **astrocyte scar** (a.k.a. **glial scar**), rich in oligodendrocytes, oligodendrocyte progenitor cells (OPCs) and fibrotic cells apart from reactive astrocytes. This glial limitans is considered as a sacrifice required to staunch extension of inflammation and tissue degeneration that compromises regeneration (Tran, Warren, & Silver 2018), albeit not being an impenetrable barrier (Lu, Jones, & Tuszynski 2007). However, the pivotal character that astrocytes have in the regeneration potential is shifting towards their positive role, as briefly discussed later. Finally, beyond the glial scar there is a **reactive and reorganizing neural tissue**. It is this tissue that holds the regeneration potential, for it contains all the elements of a functional neural tissue

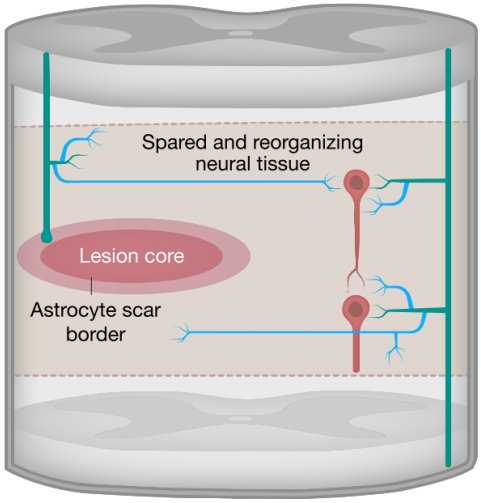

Figure 6. SCI lesion compartments (Sofroniew, 2018).

(neurons, axons, dendrites, synapses, astroglia, oligodendroglia, microglia and OPCs (Burda & Sofroniew, 2014, Tran et al., 2018).

Phases of the injury.

Upon an acute focal damage to the spinal cord, as it comes typically from trauma or ischemia, the affected and adjacent tissue enters an injury and healing process that can be organized in three stages along time (**Fig. 2**) (Burda & Sofroniew, 2014, Tran et al., 2018).

Physical trauma and primary injury: cell death and inflammation. A physical damage on the nervous tissue results in local neural necrosis and apoptosis that rapidly extends beyond the direct site of the lesion. Axons are demyelinated, retract and die back, in a process known as Wallerian degeneration (Carroll, 2009). Breaking of the blood spinal cord barrier (BSPB) leads to immediate hemorrhage, followed by vasospasm, coagulation cascades, clotting, the result being ischemia. The hemorrhage also causes edema, oxidative damage and neuronal excitotoxicity from the release of ions and neurotransmitters (e.g., Ca^{2+} and glutamate). As the scarring process advances, the tissue will be signed with abundant cavities and cysts. Activity of infiltrating M1 macrophages (Kigerl et al., 2009), oxidative stress, infiltrating ROS and iNOS and hypoxia leads to further degeneration of axons and glial apoptosis (Tran et al., 2018). Some CNS intrinsic cells respond rapidly to BSCB leakage. Alarmins

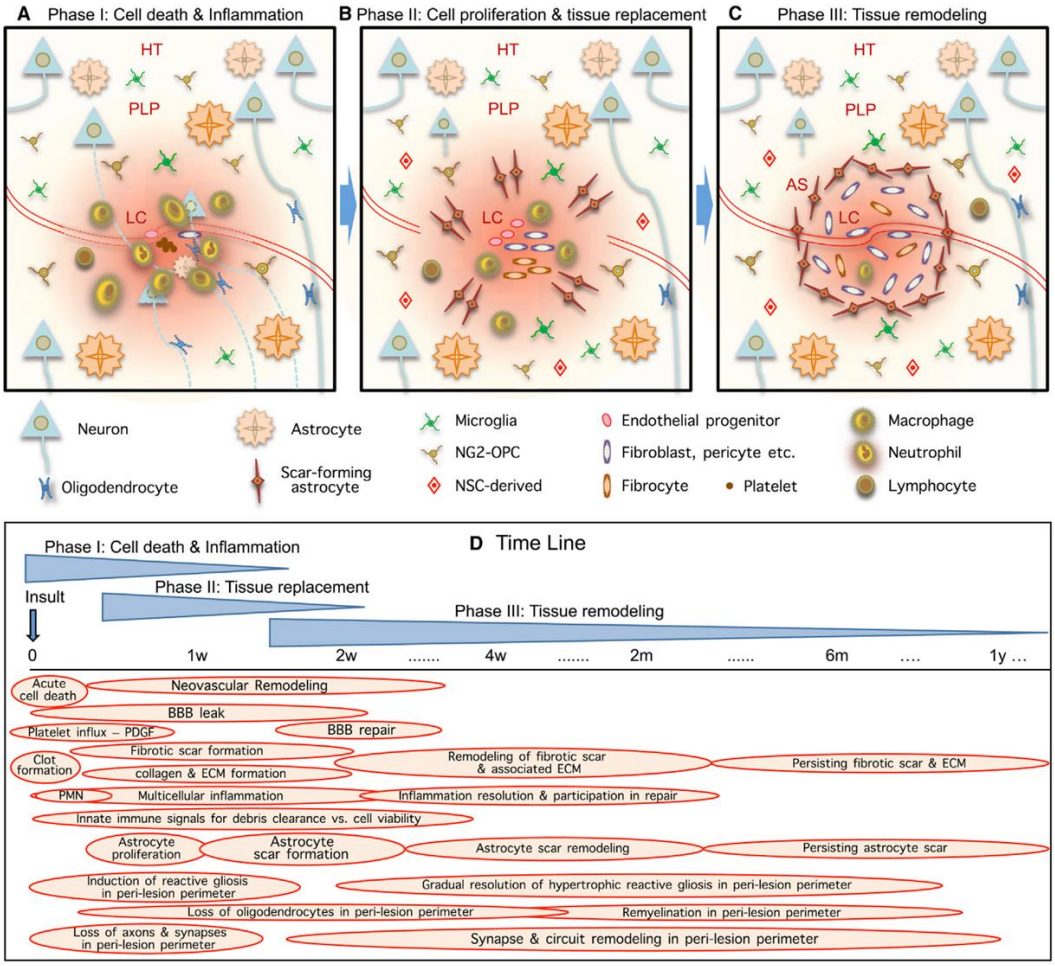

Figure 7. Phases of SCI and time course of multicellular response to acute focal CNS damage. (Burda & Sofroniew, 2014). (LC: Lesion Core, PLP: PeriLesion Perimeter, HT: Healthy Tissue, NG2-OPC: NG2-Oligodendrocyte Progenitor Cell, NSC: Neural Stem Cell)

release from cell rupture, cytokine secretion from endothelial cells and extravasating leukocytes prompt the inflammatory response.

Secondary injury: cell proliferation and tissue replacement. Inflammation induces the secondary injury that can last for weeks and results in an extension of the distorted tissue due to inflammation-induced apoptosis of neighboring cells and axotomy of survival neurons until the glial scar matures. In this phase there is migration and proliferation of cells that contribute to halt damage extension and to tissue repair, including endothelial progenitors, fibroblast-lineage cells, inflammatory cells and glial cells (Burda and Sofroniew, 2014). Whereas oligodendrocytes and NG^{2+} glia migrate to the injury site (Nimmerjahn et al., 2005) and will have a later important role in remyelination, astrocytes seem to remain in situ (Bardehle et al., 2013) and therefore, selective apparent recruitment of astrocytes would be solely due to their proliferation. Proliferating astrocytes become reactive and conform the astrocyte scar. Cell debris is cleared, there is organization of local neovasculature, formation of a fibrotic scar and the BSCB leakage is repaired. Until this happens, perfusion of endogenous and exogenous molecules is thought to drive the extension of reactive gliosis in the surrounding neural tissue. As such, this cellular proliferation migration and reorganization, together with further deposit of ECM components, shapes the definitive three-compartment organization of the injury.

Maturation of the glial scar and tissue remodeling. At last, after the new organization of the tissue has been sketched, there will be a long process of ongoing tissue remodeling. The fibrotic and astrocyte scars acquire their definitive form. Along time, there can be retraction of the lesion core and withdrawal of inflammatory elements. Importantly, the surrounding reactive neural tissue shows synapse and circuit reorganization, this being the lead for an eventual possible regeneration.

Cellular agents.

The cellular component of the injury environment is fairly complex and extends well beyond the nervous tissue functional cells. Going firstly and briefly for the non-neural cells, these include the cell types typically associated with tissue damage. Apart from their inflammatory, debris-clearance and axon retraction roles, immune cells activate the glia (Tran, Warren, & Silver 2018) and evidence accumulates supporting an active contribution of leukocytes in tissue repair (Popovich & Longbrake, 2008, London, Cohen, & Schwartz, 2013). Interestingly, macrophages shifted to the M2 phenotype do not produce axonal dieback (DePaul et al., 2015). Endothelial-related cells are drawing increasing interest (Oudega, 2012), given their trophic role in development of CNS (Dugas et al., 2008) and their synthesizing laminin, an axon growth-promoting substrate (Lein, Banker, & Higgins 1992). Fibroblasts will only appear in the CNS after injury, contributing then to the formation of the fibrotic scar given their preponderant role in the synthesis of ECM elements. Pericytes participate in the fibrotic scar, for they differentiate into a fibroblast-like phenotype and migrate to the site of the injury (Göritz et al., 2011). The deposition of a high number of fibroblasts and astrocytes gives rise to the formation of a basal lamina, with intermingled connections between these two cell types via EphB2 receptors and fibronectin-integrin matrices (Kimura-Kuroda et al., 2010). As it happens with the astrocyte scar, fibrosis helps content the extension of the lesion, but will be the cause of the chronic impairment that follows the injury, having been shown to repel axonal growth and decrease neurite length *in*

vitro (Rudge & Silver 1990) and *in vivo* (Vogelaar et al., 2015), probably due to the deposit of axon-repelling molecules (e.g., tenascin, versican, collagen) (Pasterkamp et al., 1999).

Astrocytes proliferate and become reactive upon a vast array of inflammatory and damage stimuli (e.g, Ca^{2+}, cytokines, alarmins, TGF-β). Reactive astrocytes show cellular hypertrophy, upregulation of GFAP and vimentin, hypertrophy of primary branches and expansion of normally defined astrocytic domains at the site of the injury. Due to the fact that astrocytes conform the palisade-like astrocyte barrier, they have been traditionally considered as limiting agents for axonal growth and restoration of connectivity (Reier & Houle 1988). For instance, chondroitin sulfate proteoglycans (CSPGs), an ECM component known to be detrimental for axon growth (Tran, Warren, & Silver 2018), are produced by astrocytes, although they are not the sole source and CSPG inhibition to growth is relative rather than absolute and remains controversial (Sofroniew, 2018).

Despite their border appearance, there is no evidence for astrocytes being the cause of axon regrowth failure. Instead, accumulating evidence points in the opposite direction. Any loss of functionality of astrocytes results in a major extension of the inflammation, further tissue damage and worse functional outcome (Bush et al., 1999, Faulkner et al., 2004, Wanner et al., 2013). Recently, Anderson et al. (2016) have provided strong evidence in three distinct loss-of-function mouse models and with supporting RNA-sequencing data that the astrocyte scar helps rather than hinders regeneration in the CNS. Astrocytes that form the scar are newborn cells, and it has been shown that grafts of immature astroglia can support axon growth during development and stimulate axon growth through SCI lesions (Davies et al., 2006). Additionally, astrocytes remodel the affected tissue in some positive ways, limiting edema via aquaporin expression, expressing axon growth supporting laminin, reducing neurotoxicity via glutamate transporter upregulation and limiting oxidative damage via glutathione production, and providing metabolic and trophic support for the neighboring neurons (Lukovic et al., 2014, Sofroniew, 2014, Filous & Silver, 2016).

Another important group of neural-lineage cells is conformed by $NG2^+$ OPCs and oligodendrocytes. After trauma there is oligodendrocyte depletion triggered by the secondary injury (Li, Field, & Raisman 1999), but OPCs will migrate, proliferate and accumulate in the lesion epicenter and penumbra (McTigue, Wei, & Stokes 2001). In relation with axonal growth, $NG2^+$ cells seem to colocalize with dystrophic axonal cones. The current consensus is that $NG2^+$ OPC would entrap the retracting axonal cones and stabilize them, preventing them from dying further back, although this would also prevent their regeneration (Busch et al., 2010). In a normal developmental state, synaptic-like connections between oligodendroglia and axons establish the communicating means by which oligodendrocytes can sense and resolve a demyelinating process. In the SCI context, the impediment that OPCs find to differentiate into their functional myelinating cell type impedes remyelination of axons (Totoiu & Keirstead 2005). Consequently, not only is axonal growth curtailed, but also the myelination of the axonal fibers in the site of the injury, hindering a functional regeneration.

Finally for this section, the spinal cord holds neural stem cells (NSCs) residing in the central canal that are able to respond to injury and yield progenitor cells that migrate to the lesion zone (Meletis et al., 2008a).

All in consideration, the SCI environment is deep and intertwined in terms of ECM and cell components, their roles in maturation of the injury, the influences they exert on one another and their possible potential for axon regeneration. Up to date, the lack of a concise knowledge regarding these aspects is one of the conundrums to achieve regeneration and one of the reasons why cell therapy, given the ability of cells to adapt and change their surrounding environment, may have a higher benefit, granted we still do not know precisely the roles they exert.

I. III REGENERATION: POTENTIAL AND FAILURE.

The fact that axon regrowth from CNS tissue could occur in a PNS environment, but not in the CNS, indicated that the traditionally regarded as static CNS tissue had the regenerative or growth potential, and that the realization of this one would depend more on the microenvironment that on the cell fate (Richardson, McGuinness, & Aguayo, 1980, David & Aguayo, 1981). Therefore, to understand the reversion to a developmental growth-allowing state, a potent strategy lies in comparing the situation in the PNS and in the CNS, taking into account both intrinsic neural inputs and extracellular cues. The objective of this section is not to make a thorough description, which can be encountered elsewhere (Liu, et al., 2011,van Niekerk, et al. 2016, Mahar & Cavalli, 2018), but rather to provide the view that there exists potential molecular mechanisms that make senseful the effort of developing a regenerative strategy.

After axotomy, affected neurons in the PNS initiate a cellular response that prompts a regenerative state. Pro-regenerative related genes in synapse-active neurons are silent (Quadrato & Di Giovanni 2013). Hence, after any tissue damage, there must be triggering of signaling cascades that end up bringing the neurons back to a more developmental stage. Deciphering these mechanisms is unavoidable if a precise regenerative therapy is to be achieved. In a general look, axonal damage is communicated to the soma and this responds in setting up a regenerative genetic program comprising axonal growth cone building, alterations in excitability, synthesis of proteins and activation of pathways related to axonal regeneration (van Niekerk et al., 2016).

The first cascade that occurs after injury is a rapid increase in **Ca^{2+}** that extends from the injured axon terminals to the soma. Ca^{2+} related signaling is associated to membrane repair, growth cone assembly and triggering of epigenetic modifications (Mahar & Cavalli 2018). The activation of many of the signaling cascades are dependent on this Ca^{2+} concentration. Ca^{2+} influx activates **cAMP**, which leads to a further activation of **DLK** (dual leucine zipper-bearing kinase) and **CREB1** (cAMP-responsive element binding protein 1), a proregenerative kinase and transcription factor (TF), respectively(Gao et al., 2004, Hao et al., 2016).

Apart from Ca^{2+}, there is also retrograde transport of other delayed signals along microtubules, most notable **ERKs** (extracellular signal related kinases), DLK, **JNK** (JUN-N terminal kinase) and **STAT3** (signal transducer and activator of transcription 3), all of these being associated to regeneration promotion. For instance, inhibition of ERK upstream MAP kinases and vimentin genetic deletion result in a reduced regeneration of peripheral axons (Perlson et al., 2005). These responses are themselves also dependent on the initial Ca^{2+} influx: DLK activation is mediated by cAMP, activated after increase in Ca^{2+} concentration, and ERK1 and ERK2 association with vimentin and importin-β and transport to the soma are calcium dependent. STAT3 is phosphorylated after injury by both JAKs

(Janus Kinases) and MAPKKS. pSTAT3 is then transported to the soma and imported into the nucleus, promoting neuron survival (Ben-Yaakov et al., 2012).

mTOR (mammalian target of rapamycin), is another key promotor of regeneration (Berry et al., 2016). mTOR is activated via **PI3K-Akt**. Akt additionally inactivates glycogen synthase kinase 3β (**GSK3β**). Inactivation of GSK3β also promotes axon elongation (Dill et al., 2008). **PTEN**(phosphatase and tensin homologue) is an inhibitor of PI3K and therefore, inactivation of PTEN and the other inhibitors TSC1 and TSC2 promote axonal growth both in the PNS and CNS (Abe et al. 2010, Liu et al. 2010).

In perspective, there is a general drive of signaling agents from the injured axon terminals towards the nucleus, so as to elicit the cellular response to the insult. Changes in microtubules after injury ease the retrograde transport of these molecules, and the cytoskeleton integrity is therefore a crux for successful axon regeneration (Bradke et al., 2012). As a matter of fact, axons dying back in the CNS form retraction bulbs instead of growth cones and it is thought that the former are the non-growing counterparts of the latter, growth disruption being due to microtubule inorganization (Ertürk et al., 2007). In PNS growing axons, microtubules organize in a polar orientation, the plus-end directed towards the axon terminal, establishing a drive of anterograde transport of vesicles, mRNAs, ribosomes and proteins, all of these being needed for the demanding growth cone (Verma et al. 2005, Erez et al. 2007).

Signal transduction will activate a vast array of transcription factors. Their action is not a unique one, but instead the gene regulation will be context dependent. For the topic treated here an increasing number of specific transcription factors have been related to regeneration in either the PNS, the CNS or both (see table 1 in Mahar & Cavalli, 2018 and table 1 in van Niekerk et al. 2016). In order for these TFs to have an effect over gene expression, there must be changes in chromatin organization that allow them to access. These changes are triggered also by signaling cascades and involve the nuclear export of HDACs (histone deacetylases) (Cho et al., 2013)and import of HATs (histone acetyl transferases) (Puttagunta et al., 2014), as well as the upregulation of demethylating enzymes such as TET3 (Puttagunta et al., 2014). Translocation of KAT2B histone acetyltransferase is mediated by ERK, and export of HDAC5 and HDAC3 occurs after Ca^{2+}-induced nuclear translocation of the threonine-protein kinase D1 (PRKD1) (Cho et al. 2013). Finally, the outcome is the expression of regeneration related genes, e.g. *Myc, ATF3, JUN, STAT3, Bdnf* (Mahar & Cavalli 2018). The situation is that these changes have been by far and large more abundantly been detected in the PNS, but not in the CNS. Some examples are given:

mTOR is activated in PNS but no in CNS after injury. The same happens with STAT3 (Schwaiger et al., 2000) and Atf3, Smad1 and Bdnf (Loh et al., 2017). JNK signaling induces activation of JUN and upregulates ATF3, which has been shown to be sufficient to promote regeneration in the PNS but not in the CNS (Seijffers, Mills, & Woolf 2007). Finally, after injury, there are histone acetylations (in particular H3K9 and H3K14) in the PNS, whereas in the CNS there is fail in HDAC5 histone deacetylase nuclear export and in import of the histone acetylating KAT2B (Cho et al., 2013, Puttagunta et al., 2014).

Of course, there are inhibitory pathways as well. Some molecules that activate them are Nogo, MAG (myelin associated glycoprotein) and CSPGs, which are found in the CNS after injury. These molecules cause the buildup of poly(ADP-ribose), that reduces axon growth and the activation of RHO/ROCK signaling, as treated later, with the same outcome. PTEN, an mTOR inhibitor, and SOCS3 (suppressor of cytokine signaling 3), a strong inhibitor of JAK-STAT limits axon regeneration as well (Sun et al., 2011).

Evidence is still gathering and a comprehensive, integrated and agreed view on all the signaling molecules, TFs and activated genes is lacking. However, what can be already drawn from here, with the name of some specific agents, is that the distinct intrinsic neural response to injury in the CNS is not permissive to axon regeneration due to lack of activation of transcriptional and epigenetic programs, which avoids the expression of the required genes.

The other side of the sword is the influence that the CNS microenvironment can have on neurons. At this regard, we can think of the presence of inhibitory cues and the absence of stimulatory ones, coming from both the ECM and cellular population.

Concerning growth facilitators, chemoattractant elements and growth factors that prime neurons are essential to promote a regenerative program in the tissue surrounding the lesion core. In the PNS, neurotrophins secreted by Schwann cells contribute to tissue recovery (Chen et al., 2007). In the CNS, there is no secretion of trophic factors. Some studies have shown benefits in axonal growth when some of these factors have been delivered, such as NGF (Tuszynski et al., 1994),NT-3 (Zhou et al., 2003)and BDNF (Jin et al., 2002), providing more evidence that CNS neurons retain the ability to rebuild axons if placed in the adequate environment.

Other means to achieve regeneration is the modulation of inhibitory mechanisms for synapse remodeling and axon growth. Inhibitory molecules are mainly either myelin derived, such as Nogo, oligodendrocyte-myelin glycoprotein (OMgp), myelin associated glycoprotein (MAG), Netrin-1, Eprhins and others; or ECM derived, such as CSPGs(Tran, Warren, & Silver 2018). These molecules bind to cell receptors on injured neurons and activate inhibitory transducing signals (van Niekerk et al., 2016). The PNS is devoid of these molecules and therefore cells do not have to face these obstacles.

Regarding the influence that the astrocyte scar and other cells have on this, this aspect has already been treated in the text. Nevertheless, it should be recalled that modification of the microenvironment should not solely be aimed at neurons, but also at NG^{2+} cells, astrocytes and macrophages, so that a growth-sustaining phenotype is induced in these cells.

Finally, the inflammatory response must not be left aside. Inflammation implies a more intense damage in the area of the lesion that can compromise the regenerative potential of the reactive neural tissue that surrounds the lesion core, granted it is a necessary response for the sake of the spinal cord. This being said, it is evident that a successful regenerative therapy must take into account the modulation of the inflammatory response, trying to maintain the beneficial roles of oligodendrocytes, astrocytes and M2 macrophages, while discarding the oxidative and cellular damage elicited by these cells (Tran, Warren, & Silver 2018). This can be materialized in strategies

such as blockage of proinflammatory factors, like NFκB, limiting neutrophil infiltration or introducing anti-inflammatory cytokines such as IL-4 (Francos-Quijorna et al., 2016).

All in all, despite the ongoing talking highlighting the growth potential kept in CNS neurons, the obstacles that must be surmounted to realize this potential are vast.

I. IV THERAPEUTIC STRATEGIES. FOCUS ON CELL THERAPY.

Efforts to achieve regeneration after SCI have followed a number of strategies trying to revert the impediments treated in the previous epigraph. A group can be conformed by the strategies that try to enhance the intrinsic axon regenerative ability. These strategies comprise modification of the signaling cascades and microtubule stability (Z. He & Jin 2016). Another group of strategies focus in modifying the inhibitory microenvironment. This includes modification of the myelin derived inhibitory substances, modification of the ECM and delivery of trophic factors, either via hydrogel deposits or tissue/cell engraftments of fibroblasts. Some examples are the inhibition of CSPG receptors (Shen et al. 2009, Dickendesher et al. 2012) or the degradation of CSPG applying the enzyme chondroitinase ABC (ChABC) (Starkey et al., 2012).

Cell therapy.

Most recently, during the last decade, cell-based strategies have gained a major interest as more knowledge has been acquired, particularly for stem cells. Indeed, cell transplant can modulate the microenvironment in many of these ways via secretion of trophic factors, which could drive the phenotype of oligodendrocytes and macrophages towards the M2 type, promote the intrinsic growth pathways and modulate the inhibitory cues that affect CNS tissue regeneration and provide a permissive ECM or chemoattractant molecules that foster axon growth and synapse formation. Transplanted cells, as opposite to drugs or biomaterials, can respond to signals in the injured microenvironment and alter it. However, despite the high number of assays, mechanistic insights regarding the precise action that transplanted cells exert are lacking, most certainly due to experimental limitations, standardization and critical interpretation.

The principal cell types that have been used are Schwann cells, oligodendrocyte progenitor cells (OPCs), olfactory ensheathing cells (OECs), mesenchymal stem cells (MSCs) and neural stem progenitor cells (NSPCs), all of which have rendered to a certain extent improvements in any aspect of tissue regeneration (see Table 1 in Assinck et al. 2017). The proposed mechanisms through which transplanted cells may foster regeneration are neuroprotection, immunomodulation, myelin regeneration and neuroregeneration (Assinck et al., 2017).

Neuroprotection mechanisms are those that limit the secondary damage that develops after trauma, therefore increasing the spared neural tissue around the lesion. On whether transplanted cells do promote neuroprotection, given that transplant is usually performed after two weeks or more after injury and by that time the secondary damage must already have taken place. Nevertheless, transplantation of cells has been associated to tissue sparing. One mechanism for neuroprotection is the release of cytokine and trophic factors by transplanted cells that could promote cell survival, regulate inflammation and promote vascularization, although it must be noticed that evidence remains correlative and not causative.

Immunomodulation could in fact be considered another mechanism of neuroprotection. As said before in the text, this beneficial effect implies promoting the beneficial immune action. For instance, shifting macrophage phenotypes from the inflammatory M1 to the protective M2 by multipotent adult progenitor cells (MAPCs) (DePaul et al., 2015) or by MSCs (Nakajima et al., 2012), or increasing the levels of anti-inflammatory cytokines and reducing pro-inflammatory ones (Nakajima et al., 2012).

Regarding **remyelination**, even if this is necessary for proper axonal function and Schwann cells, OPCs and NSPCs are able to increase remyelination (Pearse et al. 2004 , Keirstead et al. 2005, Plemel et al. 2014), it is still not clear whether it is remyelination itself that causes the observed functional improvements (Plemel et al., 2014).

Finally, **neuroregeneration** refers to the regrowth of nervous tissue, be it neurons, axons, synapse formation and glial cells. In a strict sense, regeneration demands functional recovery. Nevertheless, when commonly using this term in research, it will comprise statistically significant functional recovery. For neural regeneration to occur, successful connectivity in the spinal cord must be restored. This translated into either axon bridge formation across the lesion core or in formation of propriospinal relay circuits within the spared tissue (Courtine et al. 2008, Lu et al. 2012) (**Fig. 3**).Transplanted cells can conform the platform for such a bridge, not only on their own but also via secretion of axon-growth promoting molecules, i.e. laminin (Assinck et al., 2017). Also, transplanted cells can modify the astrocyte scar, turning astrocytes from their inhibitory barrier

state into a stimulatory bridge state (Williams et al., 2015), which pass to actively contribute in axon regeneration.

In any case, it must be considered that neither an apparent increase in axonal density necessarily implies axon growth or axon regeneration this term being understood as "regrowth of a transected axon" (Tuszynski and Steward, 2012), nor axon regeneration is always functionally beneficial (Takeoka et al., 2011). In this research, axon regeneration after OEC transplantation led to both hindlimb motor function improvement and worsening. At this respect, functional training is fundamental to attain functional results. Even if there is axon regrowth, one cannot assure that there will be restoration of function. Therefore, a crucial aspect for recovery after SCI is supporting the molecular and cellular strategies with rehabilitation and training (Sofroniew,

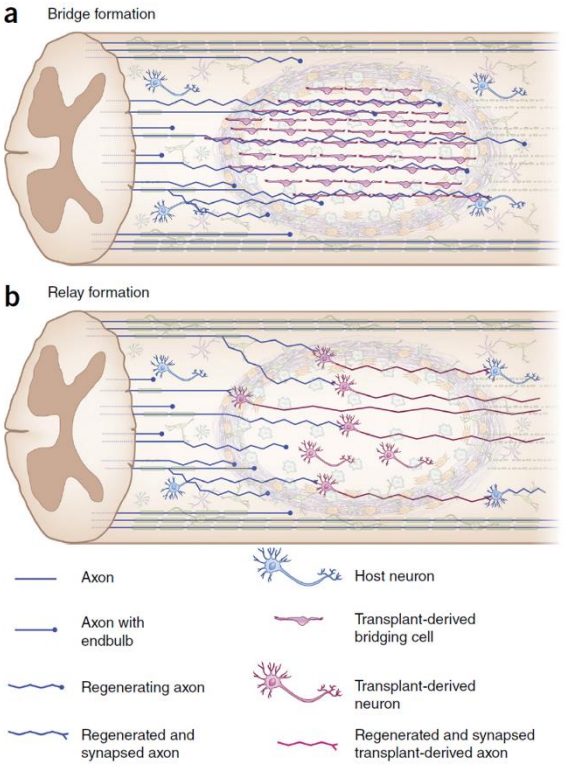

Figure 8. Repair of neural connectivity after SCI (Assinck et al., 2017).

2018). In line with this, other curative approaches work in the direction of electrical stimulation and are showing promising results (Van Den Brand et al. 2012, Capogrosso et al. 2016, Wagner et al. 2018).

I. V FOCUS ON THE PRESENT PROJECT

It goes without saying that one would fall short if aims at achieving a functional regeneration by only pulling from one string, and instead, it would be the realization of several strategies that is expected to yield a better result: combination of inhibitory stimuli blocking drugs, stimulation of intrinsic neural growth, engraftment of supportive tissue and functional training. As an example, Lu et al. (2012) combined transplant of NSPCs embedded in a fibrin matrix with 10 trophic factors and a protease inhibitor, achieving differentiation of transplanted cells that extended abundant axons along notable distances. In the same line, this project entails a combinatory cellular and pharmacological therapy using epSPCs (ependymal Stem Progenitor Cells) and fasudil, a RHO/ROCK inhibitor, either on its free form or conjugated with a polyglutamate polymer.

Cellular component: epSPCs.

epSPCs (ependymal/stem progenitor cells) are a population of adult NSCs sited at the ependymal layer of the central canal of the spinal cord. In a physiological state, epSPCs are quiescent and divide symmetrically just as a maintenance of the ependymal layer. On the contrary, OPCs show a much higher proliferating activity. However, after an event of SCI, ependymal cells are activated and become the dominant proliferating stem cell type, together with astrocytes (Meletis et al. 2008b, Barnabé-Heider et al. 2010, Lacroix et al. 2014). The progeny of epSPCs can effectively migrate to the site of the injury. Thus, stimulation of epSPC activation after injury could be a feasible strategy to ease regeneration, given their natural proximity and migration capability (Rodríguez-Jiménez et al., 2012). Interestingly, ependymal cells are the sole progenitor cells that give rise to multiple lineages in the spinal cord (Barnabé-Heider et al. 2010). Nevertheless, ependymal cell progeny mostly matures into the glial lineage, mainly astrocytes, contributing to the formation of the astrocyte scar, although they can generate a small population of oligodendrocytes as well (Barnabé-Heider et al. 2010). At this respect, a line of thought postulates driving the differentiation of ependymal cell progeny towards oligodendrocytes, arguing that the myelination these cells would exert on demyelinated axons could bring back a better functionality for the affected tissue (Franklin & French-Constant 2008). However, as it was stated before, whether myelination truly translates into functional recovery is under question (Plemel et al., 2014).

In an *in vitro* context, ependymal progenitors proliferate forming neurospheres and can indeed differentiate into diverse lineages, i.e. neurons, astrocytes and oligodendrocytes (Weiss et al. 1996, Shihabuddin, Ray, & Gage 1997, Johansson et al. 1999). It arises then the possibility of conditioning the epSPCs *in vitro* prior to transplant so as to modulate their fate once they are grafted (Moreno-Manzano et al., 2009). Additionally, the homotypic nature of the cells or tissue engrafted seems to offer a better axon growth (Kadoya et al., 2016). This could make epSPCs a better candidate to achieve bridge formation.

At this regard, the use of epSPCs as cell therapy does have shown promising results in SCI regeneration with functional recovery (Moreno-Manzano et al., 2009). But, as we were saying,

combination of cellular transplant with other strategies are expected to have a better outcome. Hence the approach followed for the *in vivo* experimental design in this project: epSPCs together with a RHO/ROCK inhibitor, whose relation with the SCI is now discussed.

Pharmacological component. Fasudil: RHO/ROCK inhibition.

The activation of RHO/ROCK signaling is strongly related to neuronal degeneration, reverse of neural growth and axon retraction. (Fujita and Yamashita 2014, Wu and Xu 2016, Koch et al. 2018). In the CNS and in the context of a SCI, there is an ample array of molecules that activate Rho via several receptors. These molecules include the myelin-derived Nogo, MAG and OMgp; LPA, polymers, such as the astrocyte-derived CSPG; RGM (Repulsive Guidance Molecule), a membrane-bound protein found in astrocytes, microglia and oligodendrocytes; ephrins, semaphorines, glutamate, cytokines and other molecules not identified (Fujita and Yamashita 2014, Wu and Xu 2016, Koch et al. 2018). The activation of Rho activates its downstream partner ROCK. This paves the way to the phosphorylation of numerous downstream molecules and thereby the induction of several cell processes that result in inflammation, decreased cell growth, stress fiber formation, actomyosin contractility, neurite retraction, induction of apoptosis and inhibition of autophagy, all this contributing to a worsening of functional recovery.

Not surprisingly, there have been abundant efforts to inhibit this pathway in neurological sciences, not only for traumatic events but also for neurodegenerative diseases, and using different strategies, such as receptor blockages, siRNA interference (Yang et al., 2013) or enzyme activity inhibition (Boato et al., 2010).

In particular, fasudil (1-(5-Isoquinolinesulfonyl)-homopiperazine hydrochloride), Y-27632 and related molecules inhibit RHO/ROCK signaling via competition for the ATP binding site of the ROCK kinase (Yamaguchi et al., 2006). There is abundant evidence of the benefits that fasudil exerts in the CNS, and also specifically for the SCI, reviewed by Wu and Xu, 2016, Koch et al., 2018. And, importantly, fasudil is a drug that can cross the blood-brain barrier and is considered as safe. There have been clinical trials (Shibuya et al., 2005) and others are ongoing (http://rock-als.uni-goettingen.de) (clinicaltrials.gov and PubMed, all entries for "fasudil, clinical, trial"). For a SCI, the compound would not be administered orally, but in the area of the lesion. In order to ameliorate the release-rate and stability of the drug, the Neuronal and Tissue regeneration and Polymer Therapeutics groups at the CIPF (Centro de Investigación Príncipe Felipe) have developed a patented version of the compound, conjugated with polyglutamate, but the effects this compound and that the conjugate can have on neural survival and axon growth have not been tested so far. In this way, fasudil and its conjugate are used as a treatment for SCI regeneration in this experiment, together with epSPC transplant.

AMPK signaling and axon growth.

The cell energetic balance regulator AMPK has been associated with neuroprotection and axonal growth, (Lin et al. 2017, Aghanoori et al. 2019). Nevertheless, it has been shown that an excessive activation of AMPK may lead to an a activation of TSC1/2 thereby inhibiting mTOR which may work in the opposite direction to axon growth (T. Williams et al. 2011, Ishizuka et al. 2013). Besides, activation of AMPK turns down energy-consuming cell processes, such as protein synthesis, and this is precisely required for axon growth (Z. He and Jin 2016). On the other hand, the stimulation of

mitochondria biogenesis by AMPK activation, another element that allows growth cone formation, could have more weight in the balance (Vaarmann et al., 2016). In this way, metformin, an AMPK molecular agonist (Rena, Hardie, & Pearson 2017) has provided protection against apoptosis in primary cortical neurons *in vitro*(El-Mir et al., 2008). In addition, AMPK and mTOR regulate autophagy via phosphorylation of ULK1 (Kim et al., 2011). Whereas AMPK-mediated phosphorylation promotes autophagy, mTOR-mediated phosphorylation suppresses it. Provided that autophagy is associated to axon growth (Clarke and Mearow 2016, Wang et al. 2018), also in the context of SCI (He et al., 2016), this constitutes another point supporting the potential benefit of activating AMPK as another molecular strategy to back axon regeneration. Hence, one of the objectives of the project is to test *in vitro* whether the effects of fasudil or its conjugate on epSPCs are mediated by AMPK.

I. VI COROLARY OF THE INTRODUCTION.

- The microenvironment found after trauma in the SCI is fraught with elements that avoid neural regeneration and restoration of function.
- The distinct cell types, both from neural and non-neural origin, contribute in a complex, intertwined manner in the restriction of the secondary damage and, in doing so, they provoke the limitation of regenerative capacities.
- Intrinsically, axon growth is regulated and requires a vast cellular machinery, which makes the development of molecular tools to boost growth cone formation a delicate issue. Pharmacological efforts have been done in this sense, aiming at the regulation of the signaling pathways.
- Cell therapy is regarded as one of the strategies that can tackle this issue most efficiently, for cells can modulate the microenvironment, modify the phenotype of glia and macrophages towards a supportive behavior, alter the astrocyte scar and provide trophic support.
- Given the difficulty of the situation and that the beneficial effects that have been encountered after use of a vast number of strategies have not been complete, combinatory and more complex strategies must be developed if a more ambitious outcome is wanted.

II. OBJECTIVES.

The hypothesis underlying the experimental design is that tackling the problem with a combinatory strategy is expected to provide a better outcome for regeneration of CNS tissue. This combinatory treatment is directed at two fronts:

(1) the modification of the deterrent microenvironment so as to render it more permissive to or even enhancing for axonal growth. Transplant of neural progenitor cells is used to pursue this objective;

(2) the modification of the intrinsic cell molecular mechanisms that impair axonal growth in the CNS. Provided the ROCK inhibitor fasudil has yielded prospective results in this direction, it is employed and a new conjugated form with polyglutamic is tested, this being expected to be more effective for having a higher stability and a steadier release in the tissue.

As part of the analysis of an experiment carried out in an *in vivo* model of SCI in *Rattus norvegicus* aiming to answer this questions, this project comprises the histological analysis of the spinal cords of these animals, which were subjected to combinatory treatments comprising transplant of epSPCs and application of fasudil, in its free and conjugated form with PGA, in order to assess if there is any sign of regeneration that could be related to the results of the functional analysis performed elsewhere. For this:

- Assess the extension of tissue degeneration on the spinal cord from the lesion.
- Assess the motor neuron population.
- Assess the extension of the glial scar.
- Assess the conservation of axonal tracts.

Additionally, in relation to the “second front”, due to the fact that a peak in AMPK activation has been after administration of fasudil, whether compromising the activation of AMPK would also compromise the axonal growth enhancement driven by fasudil is tested in *in vitro* assays on epSPCs.

III. MATERIALS AND METHODS.

III. I PART *IN VITRO*

epSPC extraction, primary culture, proliferation and differentiation.

epSPC or GFP-epSPC were harvested from neonatal (P4-6) female Sprague Dawley-Tg (GFP) 2BalRrrc rats; eGFP+/+ homozygote rats were used for in vivo experiments and eGFP−/− rats for in vitro assays. The spinal cords were dissected after complete laminectomy and the overlying meninges and blood vessels removed. The dissected tissue was cut into 1-mm^3 pieces and mechanically homogenized without enzymatic treatment in washing medium (DMEM F12, supplemented with 0.39% HEPES (Sigma), 0.05% $NaHCO_3$ (Sigma), 0.09% glucose (Sigma), penicillin and streptomycin 0.5 X (Sigma)). Samples were centrifuged at 1000 rpm for 5 minutes. Supernatant was discarded. After this, two phases remained. The lower phase contains tissue remnants. The upper one contained the cells. This upper phase was recovered in washing medium and centrifuged again to discard completely the tissue remnant.

Isolated epSPCs were cultured as neurosphere-like form in growth medium in low-attachment plates (NeuroCult™ Proliferation Medium (STEMCELL), supplemented with NeuroCult™ Proliferation Supplement (STEMCELL), 100 U/ml penicillin (Sigma), 100 µg/ml streptomycin (Sigma), 20 ng/ml EGF (Invitrogen), 20 ng/ml bFGF (Invitrogen) and 0.7 U/ml heparin (Sigma)) and 1000 µmolar NAC (Sigma).

For the assays other than the differentiation assay, epSPCs cultured as neurospheres were mechanically and enzymatically dispersed: cells were recovered from culture plaques and placed in a 15 ml Falcon tube. Cells were centrifuged at 0.3g for 5 min. Supernatant was discarded and cells were treated with Accutase (Stem Pro® Accutase, Thermo Fisher) at 37° C after soft resuspension. The enzymatic action was stopped with DMEM and cells were mechanically dispersed with the pipette. Cells were centrifuged at 0.4 g for 5 min. Cells were resuspended in culture medium (NeuroCult™ Proliferation Medium (STEMCELL), supplemented with NeuroCult™ Proliferation Supplement (STEMCELL), 100 U/ml penicillin (Sigma), 100 µg/ml streptomycin (Sigma), 20 ng/ml EGF (Invitrogen), 20 ng/ml bFGF (Invitrogen) and 0.7 U/ml heparin (Sigma)) and 1000 µmolar NAC (Sigma).

For adherent neural stem cell assays, epSPCs were cultured on Matrigel (CULTEK)coated coverslips.

Treatments

For the different treatments, compounds and their concentrations appear in **Table 1**. Cells followed a three-days treatment. In the first day, the different treatments were applied, but LPA was not added. In the second day, LPA was added. At the third day, cells were prepared for immunochemistry or recovered for protein extraction. Specific treatments appear in **Table 2** (every treatment includes NAC and this compound does not appear in the table).

LPA, it is a potent mitogen that activates RHO/ROCK pathway inducing growth cone retraction and neurite collapse (Jalink et al. 1994, Kranenburg et al. 1999). Therefore, its use in the *in vitro* model is aimed at mimicking the activation of this pathway that occurs *in vivo* after injury, in order to assess whether the application of the different treatments is able to surmount the inhibitory stimuli to

neurite outgrowth in epSPC. Fasudil, as explained in the introduction, is used to inhibit ROCK. **Metformin** is used to activate AMPK (Rena, Hardie, & Pearson 2017) and compound C is a known AMPK inhibitor.

Table 1. Compounds used in the treatment of cells.

Compound	Concentration (µ molar)	Reference
N-acetyl cysteine (NAC)	1000	Sigma
Conjugated-Fasudil (CF)	50 and 100	
Free Fasudil (FF)	50 and 100	
Compound C (CC)	10	Abcam
Metformin (Met)	100	Sigma
Lysophosphatidic acid (LPA)	10	Sigma

Table 2. Treatments for the AMPK and RHO/ROCK experiment.

Control	Met	CC
LPA	LPA-Met	LPA-CC
CC-CF50	CC-SS100	CC-FF50
CC-FF100	LPA-CC-SS50	LPA-CC-SS100
LPA-CC-FL50	LPA-CC-FF100	LPA-SS50
LPA-SS100	LPA-FL50	LPA-FL100

Immunohistochemistry

After the treatments, samples were washed x1 with PBS and fixated with paraformaldehyde (PFA) for 10 minutes, maintaining the plaques on ice and using a fume hood. Samples were washed x2 for 5 minutes each time with PBS. Next, blockage of non-specific sites was performed applying blocking solution (PBS supplemented with 5% of normal goat serum (NGS)(GIBCO) and 0.2% Triton X-100 (MERCK)) for 1 hour. The blocking solution contained PBS 5% and Triton X-100 (MERCK) 0.2% in PBS. The blocking solution was withdrawn and the solution containing the primary antibody was applied. The solution was composed of BSA 1% (Sigma) and Triton X-100 0.2%. Primary antibodies were used with a 1:400 dilution factor. An approximate volume of 70 µl was applied to each cover slide. Samples were incubated overnight at 4°C.

Prior to addition of the secondary antibody, samples were washed gently three times with PBS. Secondary antibodies were prepared with a dilution factor of 1::400 in PBS with BSA 1% and Triton. An approximate volume of 70 µL was added per cover slide and samples were incubated in darkness for 1 h at room temperature. Prior to addition of DAPI, samples were washed gently three times with PBS. DAPI (Sigma) was prepared with a dilution factor of 1:1000 in PBS. DAPI was applied for 5 minutes. Samples were washed three gently three times with PBS. Cover slides were placed and fixed on microscope slides using FluorSave™ Reagent (Millipore). Samples were stored at 4°C.

Image acquisition and measurement criteria.

Images of the samples were taken with a Leica DM6000B microscope at 20x. Images were analyzed using ImageJ. The strategies followed for the measurement of the different markers were:

Nestin: this marker was used to measure neurite growth. For each neuron, longest neurite was measured using the plugin NeuronJ.

GAP43: on the observation of the different cell morphology and marking, 6 different categories were counted: (1) extended cells with low GAP43 intensity in the soma and no observation of GAP43 in the neurites, (2) extended cells with low GAP43 intensity and observation of GAP43 in the neurites, (3) extended cells with intense GAP43 in the soma and no observation of GAP43 in the neurites, (4) extended cells with intense GAP43 in the soma and observation of GAP43 in the neurites, (5) shrunk spherical cells with no neurites and (6) shrunk spherical cells with neurites. These categories appear later in Results and Discussion in **Fig. 10**.

Casp3: this marker was used as an indicative of apoptotic cells.

Western blot.

Protein extraction was performed on ice. Culture medium was discarded and 50 µL of Lysis Buffer (50 mM Tris-HCl, 150 mM NaCl, 0,02% NaN3, 0,1% SDS, 1% NP40, 1 mM EDTA, 2 mg/mL leupeptin, 2 mg/mL aprotinin, 1 mM PMSF, 1X protease mix(Roche Diagnostics), 1X sodium orthovanadate (Thermo Fisher)) was added to lyse cells. Cells and lysis buffer were recovered, sonicated and subjected to thermal treatment at 95 °C for 5 minutes. Samples were stored at 4 °C. Protein concentration was determined via BCA assay (Pierce BCA Protein assay kit 23225, Thermo Fisher). Absorbance was measured with Perkin Elmer Wallac 1420 VICTOR2™.

To prepare the samples for electrophoresis, a volume of protein extract sample containing 30 µg of protein was mixed with 7.5 µL of DTT 1X and miliQ water up to 30 µL. Samples were heated at 95°C for 5 minutes and loaded in SDS-polyacrylamide gels (either 12% or 15%). Molecular marker used was PageRuler™ Prestained Protein Ladder (Thermo Scientific). Electrophoresis was performed at a constant voltage of 100 V for 2-3 hours. Transference was performed onto a PVDF membrane (ThermoFisher) at a constant amperage of 200 mA for 2.5 hours at room temperature. Transference efficacy was tested with Ponceau dying (P3504) and the membranes were washed in TBST (Tris-Buffered Saline (TBS)-Tween).

Membrane blocking was performed using either milk or BSA 5% in TBST for 1h at room temperature. Primary antibody incubation was performed overnight at 4 °C. Prior to secondary antibody, membranes were washed three times with TBST. Secondary antibody incubation was performed for 1h. Primary and secondary antibodies and their concentrations are listed in Table 3. Protein detection was performed using ECL Western Blot substrate (Fisher Scientific) and an automatized detection system (Amersham Imager 600 and Alliance Q9 Advanced) and (G153 Developer, G354 Fixer, Curix 60 (Agfa)).

For image quantification, the program Image Studio Lite was used or ImageJ. Protein intensity was normalized against background intensity and against tubulin intensity.

Table 3. List of antibodies used and combinations of primary and secondary antibodies.

Antibodies used for Western Blot		
Primary antibodies		
Antibody	**Dilution**	**Reference**
AMPKα	1:1000	2603 Cell Signaling
BCL2	1:1000	2870 Cell Signaling
BDNF	1:500	655114 Santa Cruz
Beclin1	1:2000	3495 Cell Signaling
Casp3	1:1000	9662 Cell Signaling
Cleaved Casp3	1:1000	96645 Cell Signaling
Lc3	1:1000	3868 Cell Signaling
pAMPKα	1:1000	2535 Cell Signaling
pCREB	1:1000	9198 Cell Signaling
PGC1α	1:1000	SC13067 Santa Cruz
pMTOR	1:1000	2971 Cell Signaling
pMYPT	1:500	Abs45 Millipore
P70 S6 kinase	1:1000	2708 Cell Signaling
pP70	1:1000	9234 Cell Signaling
Tubulin	1:1000	MAS-1603-HRP, Thermo Fisher
Antibodies used for immunocyto/histochemistry		
Casp3	1:400	9646 Cell Signaling
GAP43	1:400	128005 ABCAM
Nestin	1:400	Ab6142 ABCAM
βIII-Tubulin	1:400	MO15052 Neuromics
Secondary antibodies		
Alexa Fluor™ 555 goat anti-rabbit	1:400	Thermo Fisher
Alexa Fluor™ 647 goat anti-rabbit	1:400	Thermo Fisher
Oregon Green® 488 goat anti-mouse	1:400	Thermo Fisher

III. II PART *IN VIVO*

Maintenance of the animals, contusion, surgery, tissue preparation and staining were performed previously to my arrival at the laboratory. My involvement in the *in vivo* part of the project has comprised the histological analysis of the available material, although I participated in the capture of some new images of some slides to strengthen the available data.

Rats and spinal cord injury.

Sprague Dawley rats (~200 g) from Charles River and SD-Tg(GFP) 2BalRrrc from Rrrc (University of Missouri Columbia, Columbia, MO, USA) were bred at the Animal Experimentation Unit of the Research Institute Príncipe Felipe (Valencia, Spain). The maintenance and use of all animals were in accordance with the National Guide for the Care and Use of Experimental Animals Committee (Animal Care Committee of the Research Institute Principe Felipe) (Real Decreto 1201/2005). The rats were housed under standard temperature conditions with controlled 12-h light/ dark cycles with ad libitum access to food and water. SCI by contusion was performed as was previously described (Moreno-Manzano et al., 2009). Briefly, severe contusion (250 kdyn, “Infinite Horizon Impactor,”) at thoracic segment T8 was performed.

For chronic stage, six weeks after injury rats were treated by using an osmotic pump, Model 1007D which delivered 1 µl/h of PGA-SS-Fasudil or free Fasudil for days.

For epSPCs transplantation, 10^6 of total epSPC were transplanted intramedullary by stereotaxic distributed into rostral and caudal regions at a distance of 2 mm from the lesion at a rate of 2 µL/min by using a siliconized pulled glass pipette fitted to a 30 G Hamilton pipette and mounted on the microinjector. Rats were randomly divided into 5 groups and pharmacological and/or cellular treatments were carried out as follow:

1. Chronic Vehicle group: Rats were treated with vehicle through osmotic pump (n=6).

2. Chronic Fasudil group: Rats were treated with 10mM of Fasudil by osmotic pump for 3 days (n=6).

3. Chronic PGA-SS-Fasudil group: Rats were treated with 10mM of PGA-SS-Fasudil by osmotic pump for 3 days (n=6).

4. Chronic epSPC group: Rats were treated intramedullary injection of 10^6 of epSPC.

5. Chronic epSPC+PGA-SS-Fasudil group: Rats received a combinatory treatment of 10mM of PGA-SS-Fasudil through osmotic pump and intramedullary injection of 10^6 of epSPC.

The rats were pre-medicated with subcutaneous morphine (2.5 mg/kg) and Baytril (enrofloxacin, 5 mg/kg, Bayer, Leverkusen, Germany) and anesthetized with 2% isoflurane in a continuous oxygen flow of 1 L/min. All animals were subjected to post-surgery care and passive and active rehabilitation protocols.

Rats received subcutaneous injections of cyclosporin A (10mg/kg) starting one day prior to transplantation and administered daily.

Tissue Preparation

Rats were overdosed with sodium pentobarbital (100 mg/kg) via i.p. Rats were transcardially perfused with 0.9% saline, followed by 4% paraformaldehyde in PBS and the spinal cord tissue was cryopreserved with 30% sucrose before inclusion in Tissue-Teck OCT (Sakura Finetek U.S.A). For chronic experiment, 2.5 cm segments of spinal cord including lesion site were cut horizontally at 10µm thickness. Slices were stored at -20° C until histological processing.

Haematoxylin-Eosin Staining.

For histopathological examination by HE, staining sections for each rat were hydrated using a series of ethanol and then stained with HE solution in accordance with the manufacturer's instructions.

Immunohistochemistry.

Immunohistochemistry protocol was analogous to immunocytochemistry. PFA fixed tissue sections were permeabilized with 0.1% Triton X-100, and subsequently blocked with 5% normal goat serum in PBS. Primary antibodies were incubated overnight at 4°C. After washing, secondary antibodies were incubated for 1 hour at room temperature. All cells were counterstained by incubation with DAPI (Invitrogen). Signals were visualized by Confocal Microscopy or by APERIO Versa digital Scanner (Leica).

Sample preparation for Western Blot.

Total protein was extracted from spinal cord tissue samples. using a lysis buffer containing 50 mM Tris-HCl, pH 7.5,150 mM NaCl, 0.02% NaN3, 0.1 SDS, 1% NP40, 1 mM EDTA, 2 mg/mL leupeptin, 2

mg/mL aprotinin, 1 mM PMSF, 1 xProtease Inhibitor Cocktail (Roche Diagnostics, San Diego, CA, USA). Protein concentrations of the supernatant were determined using BCA and stored at -80C. Western Blot protocol was performed as indicated previously.

Image analysis.

Clarifying figures for the texts in this section can be found in the figures in Results and Discussion or in the Annex.

Extension of degeneration in H-E (hematoxylin-eosin). In order to assess the tissue degeneration extension, its length was measured approximately on H-E scanned images using CaseViewer (3D HISTECH) or Image Scope (Leica BioSystems). Degenerated tissue was considered until preservation of healthy structure could be observed in the central region of the slide (transversally considered, not longitudinally). It must be considered that this measure is merely approximative, due to the difficulty to visually appreciate the limit of degeneration in some slides. To normalize data for each individual animal, the mean of the measured degeneration extensions along the series of longitudinal slides was divided by the depth of the spinal cord spanning the considered cuts.

Number of motor neurons in H-E. Number of motor neurons in the longitudinal slides of the spinal cords were counted. Identification of motor neurons was done following criteria found in (Barber et al., 1984). Number of motor neurons was counted for each region corresponding to T7, T8 and T9 segments in the vertebral column, each segment measuring 4.9, 5.4 and 5 mm, respectively (Waibl, H, 1973). Localization of these segments on the images was done approximately, having as a reference the epicenter of the lesion. Not all the available slides for each animal were considered to count motor neurons. Pyramidal motor tracts, which motor neurons belong to, are found in the ventral horns of the spinal cord. Therefore, following a ventral-to-dorsal direction, slides were considered until the grey matter corresponding to the ventral horns converged. Absolute numbers of motor neurons in T7, T8 and T9 were obtained for all the measured slides in each animal. This result was normalized by the depth of the spinal cord spanning the considered cuts.

Number of NeuN+. NeuN+ cells were counted analogously to motor neurons, but with no restricting anatomical criteria. NeuN+ cells on the longitudinal slides of the spinal cords were counted for each region corresponding to the T7, T8 and T9 segments previously indicated. Additionally, the distribution of NeuN+ cells in segments measuring 0.5 mm along a total length of 12 mm centered at the lesion epicenter was obtained. For each animal, every available slide was considered. Absolute number of NeuN+ cells in T7, T8 and T9, as well as in the 0.5mm segments, for all the measured slides was obtained. This result was normalized by the depth of the spinal cord spanning the considered cuts.

Area of the glial scar. In order to assess the extension of the glial or astrocyte scar, its area was measured on combined GFAP/βIII-tubulin fluorescence images and expressed as a ratio. This ratio was calculated using two results: (1) denominator: total tissue area found in the longitudinal slide within a total length of 4mm centered at the lesion epicenter for every slide, and (2) numerator: total area of the $GFAP^-$ region (which corresponds to the area of the glial scar). This ratio was obtained for

every single slide. For each animal, the summation of these ratios was divided by the number of considered slides and these results are the ones considered for the analysis.

βIII-Tubulin$^+$ area. In order to asses conservation of axonal tracts in the region surrounding the glial scar, the βIII-Tubulin$^+$ area was assessed in a similar way to GFAP$^-$ area. In this case, ratios ware obtained in a similar way as the GFAP$^-$ area for two zones: (1) βIII-Tubulin$^+$ area in the tissue surrounding the glial scar within a total length of 4mm centered at the lesion epicenter and not including the glial scar, and (2) βIII-Tubulin$^+$ area within the glial scar. Importantly, degenerated areas, perceived with bulky, rounded shapes instead of fibrillary forms, appear as βIII-Tubulin$^+$ as well. Because of this, in each slide, the image was examined and regions of the tissue presenting this aspect were not discarded for this quantification. To obtain the value of the absolute βIII-Tubulin$^+$ area for each case, an intensity threshold was applied in ImageJ. At this respect, due to different intensity of the images and different quality arising from the IHQ procedure, the threshold values applied could slightly vary among different images. As such, threshold values varied between 100 and 150, the criterium for establishing the threshold being the conservation of fibrillar tracts in the positive area.

In the case of the tissue surrounding the glial scar, a ratio between the βIII-Tubulin$^+$ area and the total area of the tissue surrounding the glial scar was done for each slide. In the case of the tissue within the glial scar, a ratio between the βIII-Tubulin$^+$ area and the total area of the glial scar was done for each slide. For each animal the summation of these ratios was divided by the number of considered slides and these results were the ones considered for the analysis.

Statistical analysis.

Statistical analysis was performed using GraphPad Prism6. Before any statistical test, normality of the data was assayed with D'Agostino-Pearson Normality tests. In case of dual comparisons, a non-paired t-test student with a 95% confidence level was performed, either parametric or not depending on the result for the normality test. Whenever samples had a size over 30, a parametric t-test was performed independently of the D'Agostino-Pearson result. In case of multiple comparisons, a one-way ANOVA test was performed with a 95% confidence level. In case of non-parametric data, ANOVA was performed using a Kruskal-Wallis test with a 95% confidence level. Multiple comparisons between means was done with a Dunn's multiple comparison test with a 95% confidence level (p-value <0.05 *, p-value<0.01 **, p-value <0.001 ***, p-value<0.0001 ****). For statistical significance between binomial proportions StatGraphics XVIII was used.

IV. RESULTS AND DISCUSSION.

IV. I SPINAL CORD HISTOLOGICAL ANALYSIS

Neither cell therapy nor pharmacological treatment had an effect on the degeneration extension or in the number of motoneurons, either as individual treatments or in combination

The extension of secondary tissue damage in the spinal cords does not present significant differences between the different treatments (**Fig. 4A**). This is something to be expected, given that treatments were applied in a chronic situation, six weeks after injury, giving time for secondary damage to take place and for the glial scar to stabilize. Taking into account all the animals, there appears to be an aggrupation between values 5 and 10. Nevertheless, there appear two animals in the Fasudil group and one animal in the PGA group with a markedly higher affected zone, resulting in a high dispersed data. It appears that these three animals are the ones with the lowest number of measurements available, which may have biased this result. However, the three analyzed animals treated either with the conjugate (PGA-Fasudil) alone or in combination with the epSPC as well as the epSPC alone showed a global lower extension of the degenerated area with less dispersion among the data. In

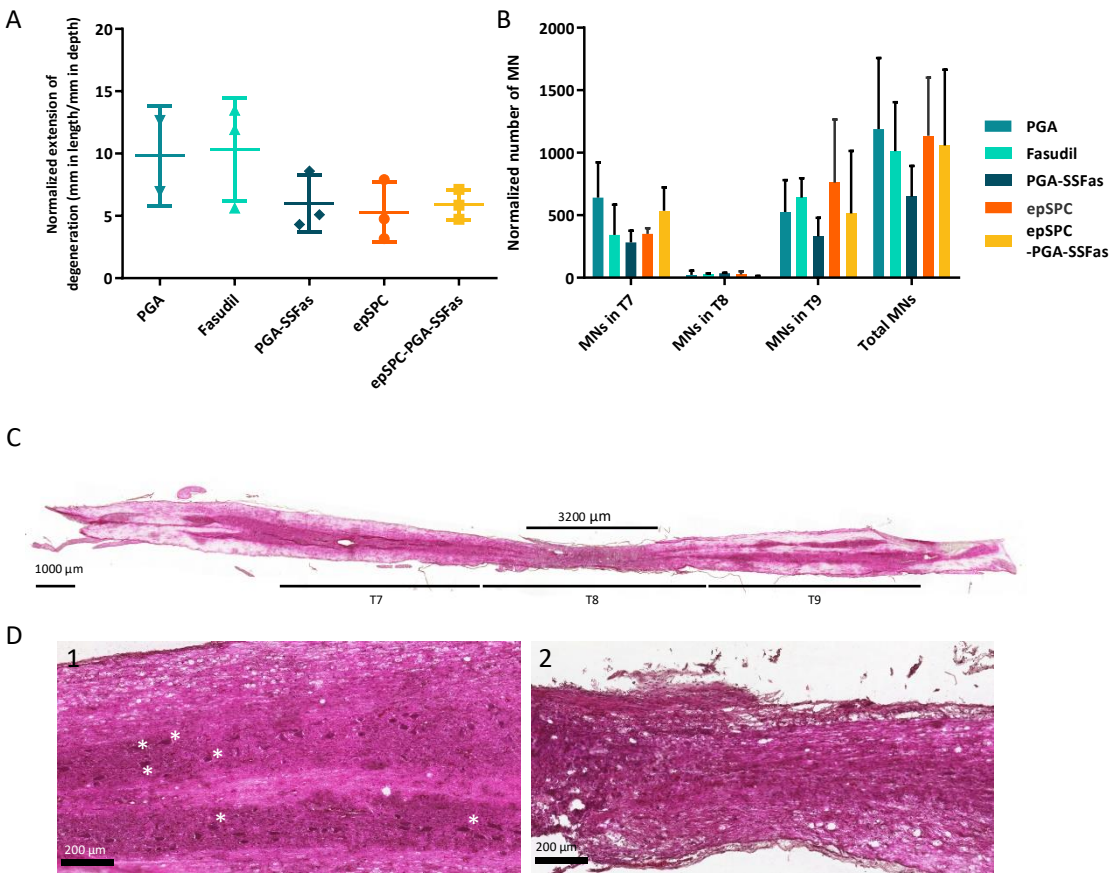

Figure 9. Extension of tissue degeneration analysis and MTN quantification at the injury epicenter, rostral and caudal segments. (A) Representation of the extension of tissue degeneration for the different treatments. No significant differences were observed. In the PGA group there are only two animals due to lack of slides from one animal. Data are normalized considering the thickness of the spinal cord spanning considered slides. **(B)** Representation of the number of motor neurons observed for the different treatments in T7, T8, T9 and the total in these three segments. **(C)** Example of one measure of degenerated tissue and localization of T7, T8 and T9 segments. **(D)** Zoom-in of a zone with conserved tissue (D1) and damaged tissue (D2) "*" indicates motor neurons. Not all are signaled. Error bars represent the SD (standard deviation). epSPC: ependymal stem/progenitor cells, MN: motor neuron, PGA: polyglutamic acid, SSFas: conjugated fasudil.

any case, there is no proof here of improvement in tissue integrity. Regarding the conservation of motor neurons, there are neither significant differences between treatments (**Fig. 4B**). In all cases, there is a quasi-inexistent population of motor neurons remaining at the site of the impact (T8), and there seems to be a higher preservation of motor neurons at the adjacent caudal zone to the lesion compared to the rostral zone, although the comparison between the number of motor neurons at T7 and T9 did not yield significant differences either. Interestingly, the lowest value for each category belongs to the PGA-SSFas group, although not significantly.

Glial scar appears enlarged in animals treated with PGA.

One of the recurrent measurements in the histological analysis for SCI regeneration is referred to the extension of the glial scar (Davies et al. 2006, Lu, Jones, & Tuszynski 2007, Anderson et al. 2016) due to the inherited vision that the astrocyte scar can limit the axonal growth, even if, as it has been said, this is a controversial notion (Lukovic et al., 2014). In any case, that the astrocyte scar limits the second-injury damaged is consolidated therefore this data is informative about the state of the tissue. For our case, the chronic state of the injury, as said before, implies that treatments will not alter the processes triggered after injury, this including the establishment of the glial scar. Because of this, any observed change, if occasioned by the treatment and not by residual factors, would indicate an *a posteriori* effect on the tissue state. This will be discussed later.

Considering our data, groups treated with PGA and PGA-SSFas show an increased $GFAP^-/GFAP^+$ area ratio as compared with the other treatments, thus presenting a worse outcome (**Fig. 5A**). Significant differences were found between the groups epSPC-PGA-SSFas and PGA-SSFas, as well as between groups Fasudil and PGA-SSFas. That is, (1) the conjugated form of the drug relates with a significantly worse outcome than the free form and (2) the conjugated form of the drug combined with progenitor cells does not present a worse outcome. Additionally, although not significant, the group treated with PGA presents a higher value for the $GFAP^-/GFAP^+$ area ratio. Taking these observations into account, what can be drawn is that grafted cells may be beneficial. Another speculation can be done, which is that there are no differences between treating the chronic animals with epSPCs, fasudil or the combination (in this case, with the conjugated form of the drug). In a simpler way, if the question is whether the use of the conjugated drug, alone or in combination with cell transplant, offers any improvement, the answer is negative for the extension of the glial scar. Additionally, one animal in the PGA group and one animal in the PGA-SSFas group have lower values, similar to those of the other treatments (**Supplementary Fig. 1**).

No differences were found for the conservation of axonal tracts among treatments.

Another aspect that is analyzed is the conservation of axonal tracts (Sun et al., 2011, Lu et al., 2012, Anderson et al., 2016, M. He et al., 2016) In this case, it has been done marking cells with the neuron marker β-III tubulin. A higher ratio indicates a better tissue integrity. Two regions have been measured independently: the tissue within the glial scar and the tissue surrounding the glial scar (**Fig. 5D**).

For the former, values are not significantly different between treatments (Fig. 5B). This means that for all cases the conservation of axonal tracts, or more precisely said, the fraction of β-III tubulin$^+$ area, within the glia scar is in a same state. In the case of the tissue surrounding the glial scar, there appears significant differences between epSPC and epSPC-PGA-SSFas groups, as well as between epSPC-PGA-SSFas and PGA-SSFas groups (Fig. 5C). The lowest value is found in the epSPC-PGA-SSFas group. However, these animals had a lower extension of degeneration (Fig. 4A). On the contrary, the higher value present in the PGA-SSFas group contrasts with the worse motor neuron conservation of this group (Fig. 4B) and the higher GFAP$^-$/GFAP$^+$ area ratio. As a matter of fact, two animals in this group (PGA-SSFas), presented extended GFAP$^-$ areas within the 4mm section of the spinal cord considered to make the measurement. This implies that little room was left within this 4mm section for tissue surrounding the glial scar, which may well have biased the values obtained. In the case of the epSPC group, not only does it present a higher β-III tubulin$^+$ area ratio (Fig. 5C), but also has a

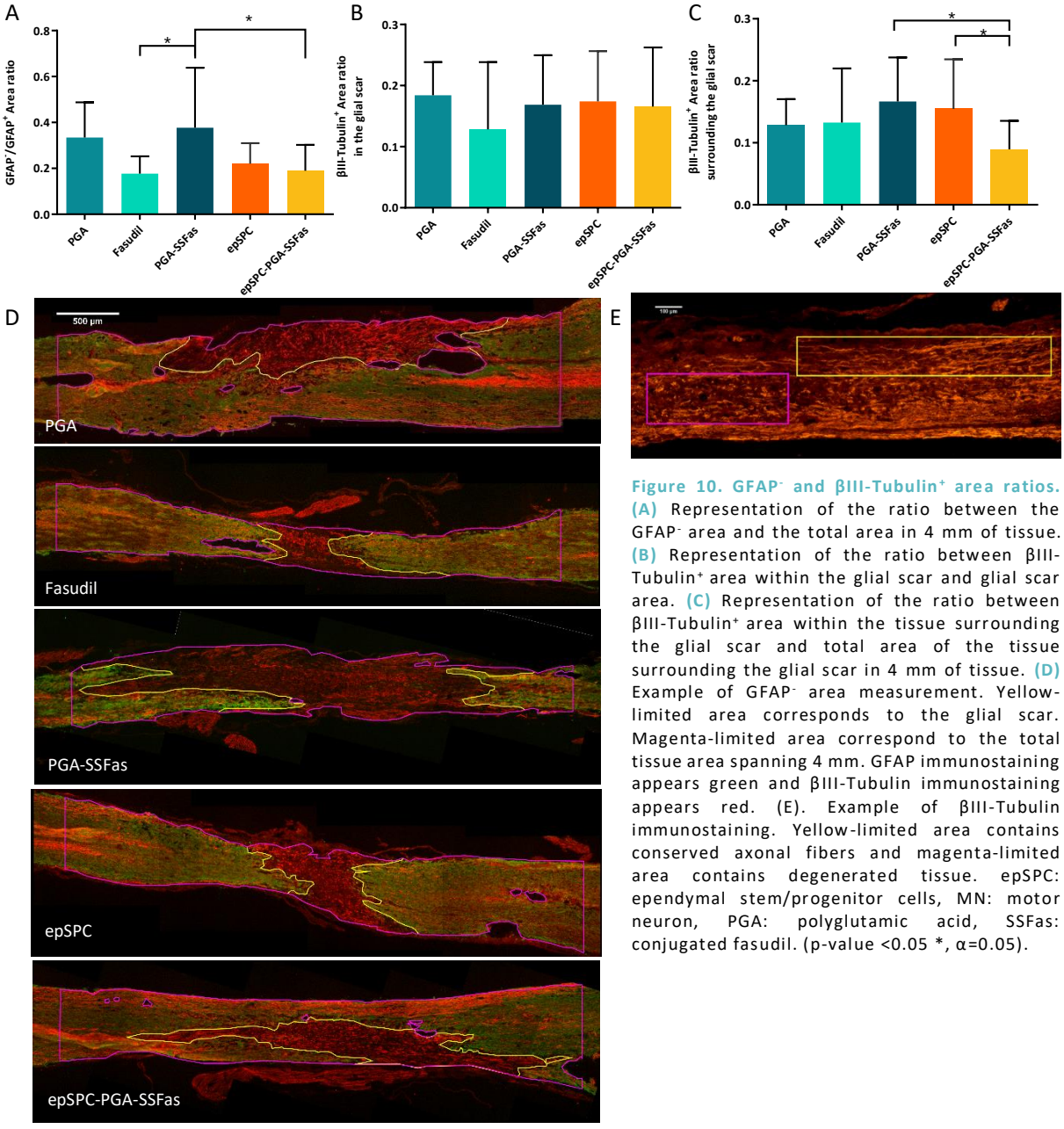

Figure 10. GFAP$^-$ and βIII-Tubulin$^+$ area ratios. (A) Representation of the ratio between the GFAP$^-$ area and the total area in 4 mm of tissue. (B) Representation of the ratio between βIII-Tubulin$^+$ area within the glial scar and glial scar area. (C) Representation of the ratio between βIII-Tubulin$^+$ area within the tissue surrounding the glial scar and total area of the tissue surrounding the glial scar in 4 mm of tissue. (D) Example of GFAP$^-$ area measurement. Yellow-limited area corresponds to the glial scar. Magenta-limited area correspond to the total tissue area spanning 4 mm. GFAP immunostaining appears green and βIII-Tubulin immunostaining appears red. (E). Example of βIII-Tubulin immunostaining. Yellow-limited area contains conserved axonal fibers and magenta-limited area contains degenerated tissue. epSPC: ependymal stem/progenitor cells, MN: motor neuron, PGA: polyglutamic acid, SSFas: conjugated fasudil. (p-value <0.05 *, α=0.05).

lower $GFAP^-/GFAP^+$ area ratio (**Fig. 5A**) and a lower extension of degeneration (**Fig. 4A**). So far, all these facts go in the same direction and support a better performance of the rats treated solely with progenitor cells.

Control animals show a better neural lineage cell conservation, although not significantly.

NeuN is a protein localized mostly in the nucleus, and partially in the perinuclear cytoplasm, expressed in the vast majority of differentiated post-mitotic neuronal cells. Therefore, it can be used to quantify the conservation of the neural lineage in the tissue after the SCI (Gusel'nikova & Korzhevskiy 2015). Just to note, one of the neuron types that are not marked by NeuN are γ-motor neurons (Gusel'nikova & Korzhevskiy 2015), which are also found in the anterior grey columns. Results are presented as the total number of $NeuN^+$ cells observed by vertebral segments (**Fig. 6A**) and distributed in sections of 0.5mm long (**Fig. 6B-F**). Considering the gross quantification by vertebral segments, there is no survival or regrowth of neurons in the contusion area (T8). Whether there is a tendency for a higher conservation of neurons rostrally or caudally to the lesion, this cannot be stated considering all the treatments (no significant difference was found). Examining the $NeuN^+$ cell distributions (**Fig. 6B-F**), in a general view, their numbers begin to increase at around 2mm away from the lesion center. Examining the behavior according to treatments, both Fasudil and PGA have a similar higher rostral distribution of $NeuN^+$ cells, although only one animal could be considered from the Fasudil group and one of the animals in the PGA group show a much lower population of $NeuN^+$ cells.

Introducing other types of analysis, more conclusions can be obtained from these data. There is not an apparent correlation between the number of $NeuN^+$ cells and the extension of the degenerated tissue, when all animals are considered (**Fig. 7A**). That is, one would expect that, provided a higher region of the tissue is degenerated, a higher number of neural cells will have died and therefore a lower number of $NeuN^+$ cells would remain in the tissue. As such, a negative correlation could appear, but this has not been the case. If we consider the global distribution of $Neun^+$ cells not longitudinally but transversally, they do increase as we move in a ventral to dorsal direction (**Fig. 7B**), to the simple major presence of grey matter. From the longitudinal distributions of $NeuN^+$ cells (**Fig. 6**), an approximate $NeuN^-$ region could be obtained and compared with the extension of tissue degeneration measured on the HE staining (**Fig. 7C**). No correlation could be established between the extension of $NeuN^-$ tissue and the extension of degenerated tissue either but for the PGA group, which showed a positive correlation. That is, for these animals, a higher extension of damaged meant a vaster region without neural cells. It was also analyzed whether the extension of the $NeuN^-$ area was higher, equal or lower than the extension of the tissue degeneration (**Fig. 7D**). A ratio >1 would indicate that neuronal death extended beyond the secondary damage; a ratio <1 would indicate conservation of neurons within the degenerated tissue; and a ratio =1 would indicate the identity between both parameters. The ratio is not significantly different from 1 for any case but for the case of PGA, in concomitance with the elevated population of $NeuN^+$ cells shown (**Fig. 6A**) and the positive correlation (**Fig. 7C**). This means that there has been a higher conservation of neural cells. Even if the PGA group has been highlighted in several results, it must be kept in mind that these results come from the same raw data looked from different perspectives.

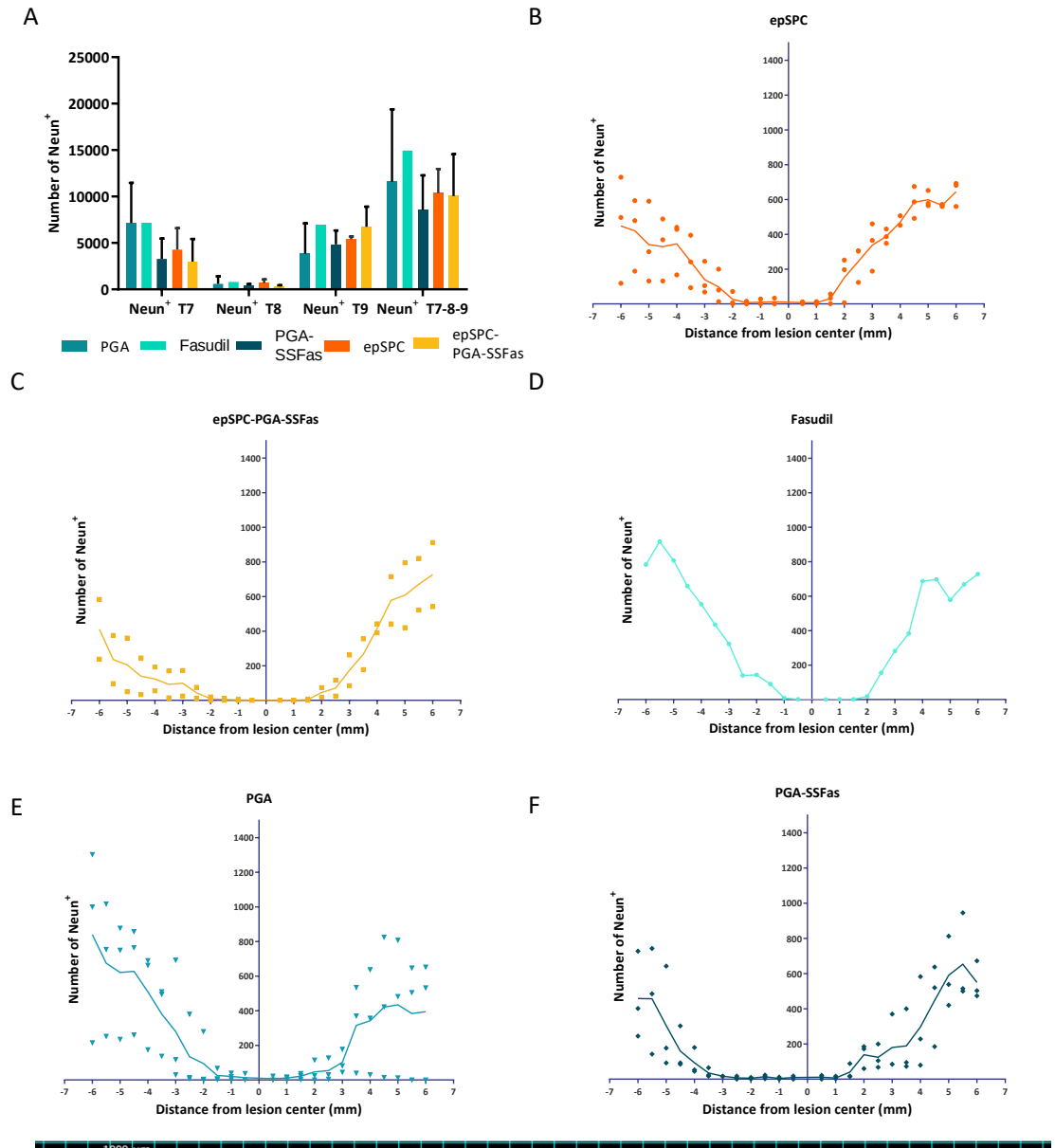

Figure 11. Distribution OF NeuN⁺ cells (A) Representation of the number of NeuN⁺ cells observed for the different treatments in T7, T8, T9 and the total in these three segments. No significant differences between treatments were observed. Error bars represent SD. **(B-F)** Representation of the NeuN+ cell distribution for the different treatments. Dots represent raw data from each animal. The continuous line represents the mean value. **(G)**Example of a tissue slide with NeuN immunostaining. **(H)** Localization of T7-T8-T9 segments and division of the tissue in 0.5x0.5 mm2 squares for distribution quantification. **(I)**Zoom-in of (H)showing individual NeuN+ cells. Arrows indicate NeuN+ cells (not all are indicated). epSPC: ependymal stem/progenitor cells, MN: motor neuron, PGA: polyglutamic acid, SSFas: indicate NeuN+ cells (not all are indicated). epSPC: ependymal stem/progenitor cells, MN: motor neuron, PGA: polyglutamic acid, SSFas: conjugated fasudil.

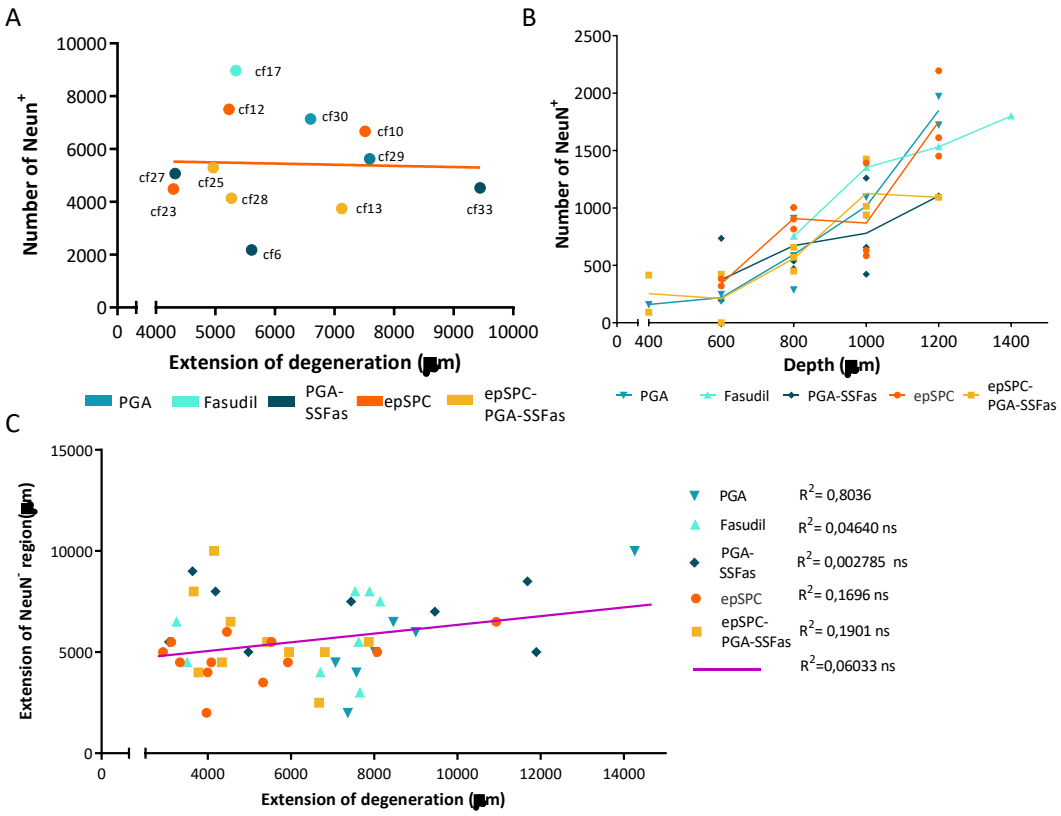

Figure 7. Degenerated tissue extension and NeuN⁻region comparison (A) Extension of degeneration vs Number of Neun⁺ cells in the total extension of the tissue. R^2= 01,3E-3. ns from 0. **(B)** Number of NeuN⁺ cells along depth of the spinal cord in a ventral-to-dorsal direction. For each animal and treatment, the total number of NeuN⁺ cells found at a given depth is represented. **(C)** Extension of degeneration vs extension of NeuN- region. Only animals from the PGA group exhibit a positive correlation significantly different from 0. **(D)** Ratio between the extension of the NeuN⁻ area over the extension of tissue degeneration. No significant differences were found between groups. Only the PGA group was found to be significantly different to 1 (*). epSPC: ependymal stem/progenitor cells, MN: motor neuron, PGA: polyglutamic acid, SSFas: conjugated fasudil. "cf+number" refers to each animal.

Conjugated fasudil strongly inactivates RHO/ROCK.

Considering the activation of the RHO/ROCK pathway, one method of testing this is the phosphorylation of the protein myosin phosphatase (P.-Y. Liu & Liao 2008). Besides, phosphorylation of myosin phosphatase in the context of axonal growth impairs the formation of the axonal cone (Tan et al., 2011). As a ROCK inhibitor, fasudil is expected to reduce the levels detected of pMYPT. Results show that samples from animals treated with transplant of epSPCs (either alone or in combination with the conjugated form of Fasudil) do not present a marked reduction in pMYPT. As a fact, one of the samples from the epSPC group presented a 4-fold increment with respect to the control. This is in concomitance with the fact that these animals (group epSPC) did not receive the ROCK inhibitor. But the other animals, which did receive fasudil (group epSPC-PGA-SSFas) have not presented a lower presence of pMYPT.

On the contrary, samples from animals treated only with fasudil, either free or conjugated, do present a marked reduction in pMYPT as compared to the control. When comparing the means of these two groups (Fasudil and PGA-SSFasudil), the value for the fasudil group is 3 times higher than that of the PGA-SSFas group. Therefore, (1) administration of the drug did induce inactivation of the RHO/ROCK pathway, as expected (although not when administered together with cell transplant) and (2) so does the conjugated fasudil when compared to its free form.

An similar scenario is found when looking the relative levels of pAMPK/AMPK. Treatments comprising only fasudil have a higher ratio, in concordance with previous results obtained by the group, consisting in this observation on AMPK activation *in vivo* after fasudil administration. Treatments including progenitor cells show a lower ratio, also in the group treated with both conjugated fasudil and cell transplant.

Summing up these results, treatment with fasudil did inactivate RHO/ROCK and activated AMPK, whereas this cannot be stated for transplant of progenitor cells. Additionally, in the combinatory treatment, fasudil has not had these effects and therefore, perhaps transplanted cells are somehow impairing the molecular action of the drug.

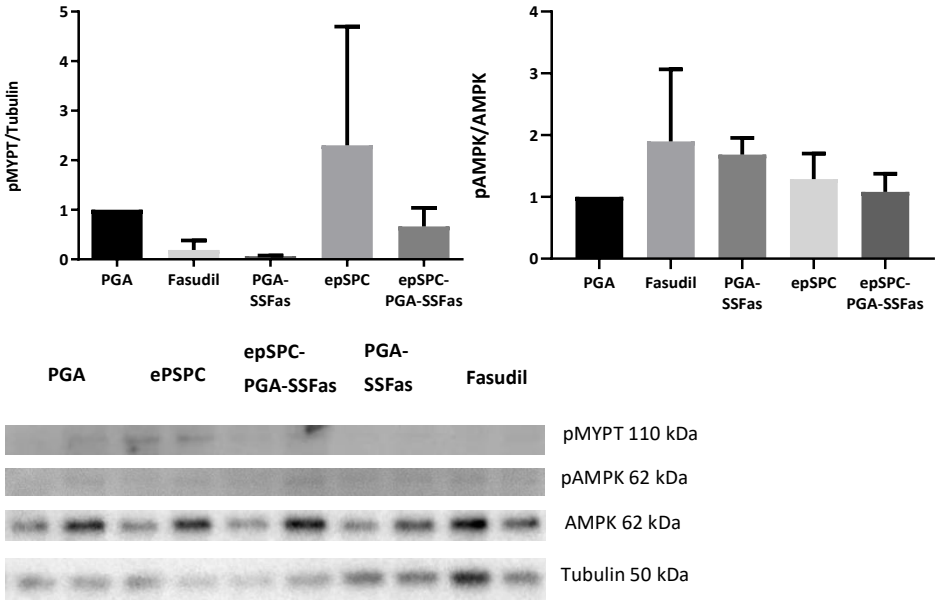

Figure 8. RHO/ROCK and AMPK activation in rats with a chronic SCI. Error bars correspond to the SD of the two samples loaded in the gel for each treatment. Each sample came from a different animal. epSPC: ependymal stem/progenitor cells, PGA: polyglutamic acid, SSFas: conjugated fasudil.

Taking all into account.

Evident differences have been found for the RHO/ROCK signaling between treatments, with the strongest inhibition been exhibited by the conjugated fasudil. This could indicate that during the three weeks between the beginning of treatment and the sacrifice of the rats, the polymer conjugate may have allowed a better conservation of fasudil in the tissue. This affirmation supports the initial purpose of developing a more stable conjugated form of the drug, which was offering a more sustained effective treatment for a long period. As said in the introduction and supported by

evidence (Wu & Xu, 2016, Koch et al., 2018), it should be expected an increased axonal growth in cases where RHO/ROCK is inhibited. Unluckily, this could not be corroborated in the histological analysis. To look for this, the axonal tracts marked with βIII-tubulin are the target to analyze. However, limitations inherent to the techniques used for our case, a confident result could not be obtained for the conservation of axonal tracts. At this regard, Sun et al.(2011) performed a nice approach on axonal tract conservation via quantification of the estimated number of regenerating axons along the distance from the lesion. Nevertheless, the group PGA-SSFas, which is the one with the strongest RHO/ROCK inhibition (**Fig. 8**) was also the one with the highest βIII-tubulin^{+} area ratio. Notwithstanding, because the epSPC group (with a high RHO/ROCK level) also exhibited a higher βIII-tubulin^{+} area ratio and we have also warned that precisely the tissue in PGA-SSFas animals had a more extended glial scar. As a last note in relation with this, I recall that neither an apparent increase in axonal density necessarily implies axon growth or axon regeneration (Tuszynski and Steward, 2012), nor axon regeneration is always functionally beneficial (Takeoka et al., 2011).

In regard to AMPK activation, its participation in promotion of axonal growth is still not precisely defined, despite its beneficial effects in neuroprotection (Lin et al. 2017, Aghanoori et al. 2019) and activation of cellular processes that can support growth of axons, such as protection against apoptosis (El-Mir et al., 2008) or autophagy induction (He et al., 2016). If we consider the premise of "AMPK activation is neuroprotective", it is found that treatment with fasudil exerts a positive effect in this direction (**Fig. 8**). However, we find again that this is not translated into the histological examination. In this case, motor neuron conservation and neural cell conservation would be the most informative assessments. However, the histological analysis for these aspects was not conclusive either (**Fig. 4B, Fig. 6, Fig. 7**).

It must be said that there were other analysis that could not be carried out on time. For the molecular signaling, pathways that are pertinent to analyze are those involved in apoptosis and autophagy. In order to better characterize axonal growth, mTOR, Akt, GSK3β and PTEN expression examination would have been relevant, as explained in the introduction. Given the tendency that epSPCs have shown to mature into oligodendrocytes (Moreno-Manzano et al., 2009) and the alleged beneficial role these would have on the lesion remyelination (Pearse et al. 2004 , Keirstead et al. 2005, Plemel et al. 2014), another measurement that was previewed was the population of oligodendrocytes close to the lesion epicenter. Another analysis that would have been convenient is the permanence and migration of transplanted cells, which could be detected given they express GFP. For a better characterization of the glial scar, or whether there were signs of modification of the astrocyte barrier, some papers refer to a change in astrocytes from a wall-like restraining to a bridge-like permissive morphology (Sun et al., 2011, Zukor et al., 2013, R. R. Williams et al., 2015).

Now, it could be assumed that the signs of regeneration were not found in the histological analysis due to the chronic character of the injury and the brief time between start of the treatment and sacrifice (3 weeks), but there is evidence of axonal regeneration in chronic SCIs (Houle, 1991, Romero, Rangappa, Garry, & Smith, 2001). Very interestingly, Yokota et al., (2019) use an almost equal tissue preparation to the one carried out by our group, but they adopt other approaches. First, they were able to make a 3D reconstruction and assess the synaptic activity both with

immunolabelling and gene expression of motor neurons isolated with laser microdissection. However, they did not trouble themselves analyzing axonal tract conservation and length. Finally, labelling techniques other than immunolabelling can be used. Tract tracing is considered the gold-standard for the identification of specific axonal tracts (Tuszynski and Steward, 2012) and they offer a great anatomical detail. As it happens with other fields, transgenic animals marked for specific cell types can be sued (Bareyre et al., 2005), which can offer axonal marking without the need of transport that requires axonal tracing. Finally, the recently-developed CLARITY technique for tissue clarification does allow the ultimate detailed 3D reconstruction of nervous tissue, to the level of being able to tract single axons for long distances (Chung and Deisseroth, 2013).

At last, in the current project, one has the sensation that animals bearing a chronic condition behave similarly in response to the treatments, despite the differences observed in the WB experiment. A more precise and abundant histological analysis would be required and a higher number of individuals to strengthen the confidence of these results.

IV. !! ASSESSMENT OF THE INFLUENCE OF AMPK OVER THE ENHANCEMENT OF NEURITE OUTGROWTH BY FASUDIL/PGA-SSFASUDIL-MEDIATED ROCK INHIBITION.

Experimental data obtained in the laboratory have shown that, after administration of fasudil *in vivo* there is a peak in the activation of AMPK and an increase in the levels of cAMP. The question arises then, whether AMPK is involved in the activation of axonal growth when RHO/ROCK is inhibited with fasudil: Is the drug still able to promote axonal outgrowth when AMPK is inhibited? This has been tested in an *in vitro* experiment on epSPCs with two conditions: (1) when RHO/ROCK is not activated by any exogenous cue (**Fig. 9A, C**) and when RHO/ROCK is activated by an exogenous cue, LPA (**Fig. 9B, D**); and two variables: neurite length and expression of GAP43.In order to compare fasudil treatments with AMPK activation or inactivation, metformin (Met) and compound C (CC) have been used (see introduction).

AMPK inactivation does not impair neurite length increase driven by fasudil.

First all, when comparing the treatments without fasudil (Met, CC, LPA, LPA-Met and LPA-CC) (**Fig. 9A, B**) with the control, no significant differences appear, with the exception of Met. However, the experiment was carried out twice and neurite length comparison between the control group and the Met group was significant in only one of them. Additionally, there are no significant differences between the Met and CC groups. Importantly, LPA, which is a known RHO/ROCK, has not shown a significantly lower neurite length as compared to control. This can be due either to the fact that the compoundd failed, or that control cells did not differentiate enough to develop neural processes and therefore LPA had no cellular process to inhibit. Therefore, it will be assumed that these treatments, on their own, do not alter axonal growth, either in a positive or negative sense.

We will analyze the behavior of fasudil , free and conjugated, treatments first with respect to controls. Later, differences between fasudil treatments will be mentioned.

When treatments without RHO/ROCK activation are considered (**Fig. 9B, D**), it is seen that fasudil either free or conjugated and at a lower or higher doses significantly increases neurite length compared to control, as it has already been proved for the free form(Wu and Xu 2016, Koch et al.

2018). Therefore, the new form of the drug seems to be also uptaken by epSPCs and promote neurite outgrowth. Significant differences have been also obtained when comparing cells treated only with

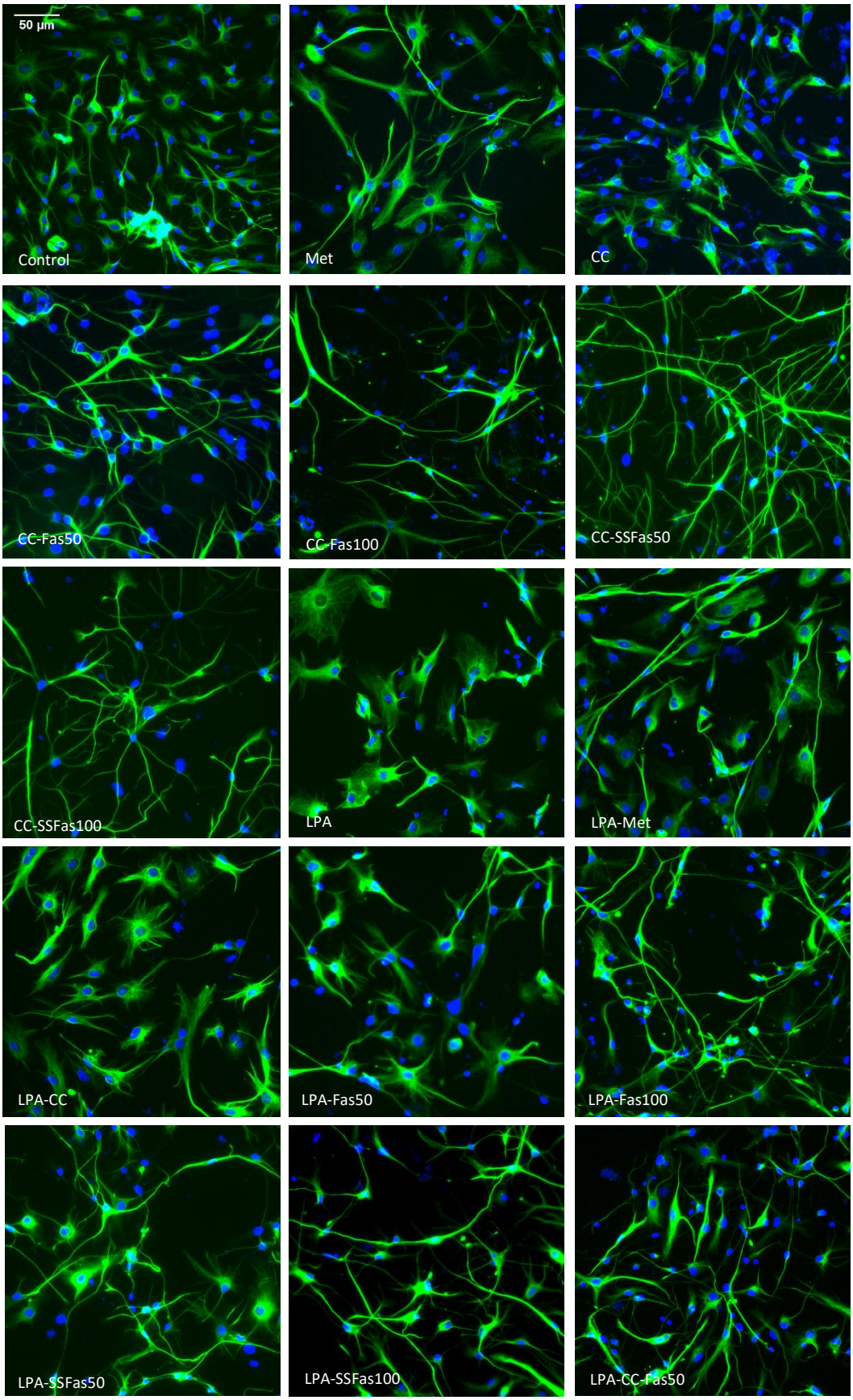

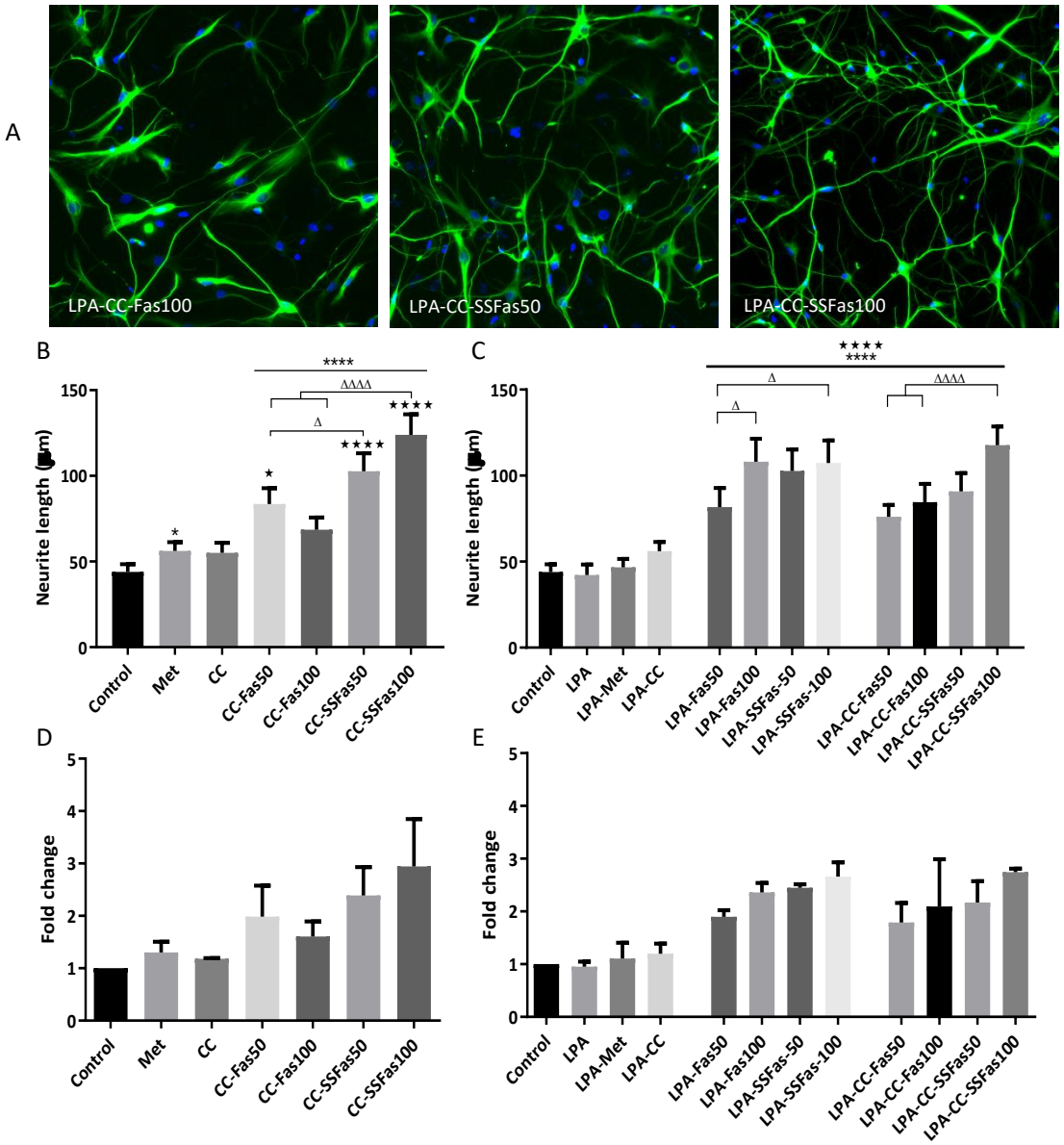

Figure 9. Neurite length of treated epSPCs. (A) Snapshots of cells showing different morphology. **(B, C)** Representation of neurite length mean for treatments without LPA and with LPA. **(D, E)** Representation of fold change in neurite length with respect to the control for treatments without LPA and with LPA. LPA: lysophosphatidic acid, Met: Metformin, CC: Compound C, Fas50: Fasudil at 50 µmolar, Fas100: Fasudil at 100 µmolar, SSFas50: conjugated fasudil at 50 µmolar, SSFas100: conjugated fasudil at 100 µmolar. (* significant to control, * significant to Met, Δ significant between indicated groups; p-value <0.05 *, p-value<0.01 **, p-value <0.001 ***, p-value<0.0001 ****, α=0.05))

metformin. It is true that treatment with free fasudil at 100 µmolar has not yielded a significant increase. However, in the other cases when fasudil 100 µmolar has been used (**Fig. 9B**), it did have induced a significant axonal growth. The information in this paragraph can be interpreted as follows: when RHO/ROCK is not activated and when AMPK is inactivated, the compound is still able to enhance axonal growth. This supports the affirmation that AMPK signaling does not interfere with induction of axonal growth via RHO/ROCK inactivation.

When treatments with RHO/ROCK inactivation are considered, a similar outcome is observed (**Fig. 9 B, D**). Every treatment including fasudil (free or conjugated) significantly increases neurite length as compared both to control and LPA-Met groups. This is true either when AMPK is inhibited or not.

These results shed more evidence in the direction just stated: that AMPK inactivation does not impair axonal growth induction by fasudil, even when RHO/ROCK is activated.

Finally, whether the conjugated fasudil was able to stimulate axonal growth more intensely than the free form under AMPK inactivation is now addressed. Our starting position is that the conjugated form does show a better performance than the free form (experimental data obtained in the laboratory). For the data presented here (**Fig. 9B**), we find that only at a dose of 100 µmolar does the conjugated form stimulates axonal growth in a significantly higher way than free fasudil when AMPK is inhibited (LPA-CC-SSFas100 against LPA-CC-Fas50 and LPA-CC-Fas100 on the figure). Nevertheless, this is merely in line with the repeating observation that the conjugated form shows a better performance *in vitro.* A different situation would have been, for instance, that the free form did not yield significantly different results from control when AMPK is inhibited but that the conjugated form did.

Gathering this information into one sentence, as said in the title of this epigraph: AMPK inactivation does not impair neurite length increase driven by fasudil (free or conjugated) and conjugated fasudil is also able to promote neurite outgrowth.

Fasudil induces expression of GAP43 and localization on the growing axons.

GAP43 is a protein associated to axonal growth whose expression is limited to neural cells, although it has also been reported to be slightly expressed in neonatal rat cortical astrocytes (da Cunha et al., 1991). It localizes intensely in presynaptic terminals in both peripheral and central nervous systems (Holahan, 2017) and in growing neurons *in vitro*, exhibits a diffuse expression throughout the soma and appears with a high intensity in neurites, usually in a punctuate manner(Donnelly et al., 2013). It has been found that GAP43 mRNA is stabilized by the Hub protein, and then transported to the axonal tip (Yoo et al., 2013). GAP43 is thought to mediate axonal growth via modification of the terminal structure of the axonal end (Holahan, 2015). In particular, GAP43 supports accumulation of F-actin filaments at the growth cone (Laux et al., 2000). As such, in neurons with an active process of axonal growth, a stronger expression of GAP43 in neurites is expected.

For our case, epSPCs were immunostained against GAP43. on the observation of the different cell morphology and marking, 6 different categories were counted (**Fig. 10**):

- type 1: extended cells with low GAP43 intensity and observation of GAP43 in the neurites,
- type 2: extended cells with intense GAP43 in the soma and observation of GAP43 in the neurites,
- type 3: shrunk spherical cells with neurites.
- type 4: extended cells with low GAP43 intensity in the soma and no observation of GAP43 in the neurites,
- type 5 extended cells with intense GAP43 in the soma and no observation of GAP43 in the neurites,
- type 6: shrunk spherical cells with no neurites. Most likely dead cells.

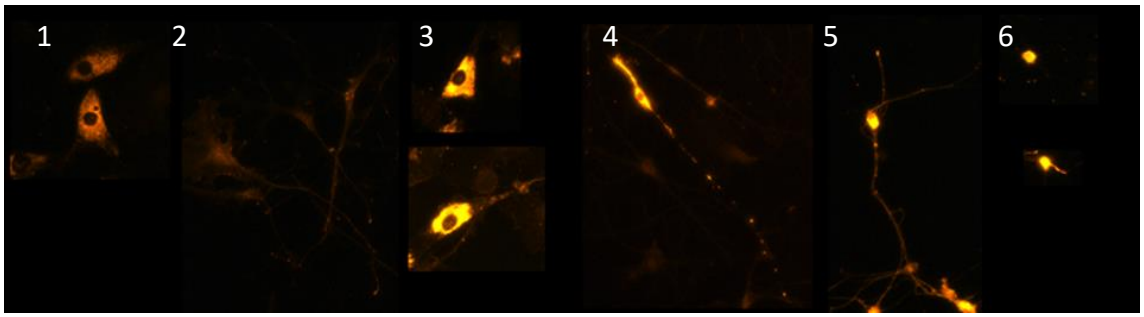

Figure 10. Six morphologies distinguished based on GAP43 immunostaining

In relation to axonal growth, types 1, 2 and 3 are the ones that were considered. Treatments without LPA are going to be commented first and next, treatments with LPA. When regarding the $GAP43^+$ proportion of type 1, 2 and 3 for treatments with no induced RHO/ROCK activation (**Fig. 11 B**), first of all, activation of AMPK by metformin did not results into a higher GAP43 expression, although its inhibition did have the opposite effect, the proportion of $GAP43^+$ cells being significantly lower than the control. This raises the first question regarding whether the cellular processes enhanced by active AMPK may affect transport of GAP43 or GAP43 mRNA to the growth cones. Secondly, all treatments including fasudil resulted into a significantly higher GAP43+ expression when compared to both control and Met groups. Therefore, AMPK did not seem to interfere with the fasudil-driven GAP43 expression increase.

Considering groups treated with LPA (**Fig. 11C**), in this case, regarding the action of metformin, whereas LPA and LPA-CC groups were showed no significant difference with the control, the LPA-Met group did, with a higher $GAP43^+$ cell proportion. The question that falls is whether activation of AMPK becomes more relevant when RHO/ROCK signaling is enhanced, although this perhaps makes not too much sense, provided that LPA is working against axonal growth and treatment with metformin alone did not result into a higher GAP43 expression. When observing groups treated with fasudil, either with AMPK inhibition or without it, all of them show a significantly increased $GAP43^+$ cell proportion with respect to the control group. However, the comparison for these groups is established with the LPA-Met group, only three fasudil treatments yielded a significant increase: LPA-SSFas50, LPA-CC-Fas100 and LPA-CC-FasSS50. From here, several observations can be drawn: (1) the conjugated form of the drug seems to exhibit a better performance to enhance GAP43 expression than the free form, which is in concomitance with the higher neurite length observed for cells treated with the conjugated form (**Fig. 9**); (2) this effect is dose-dependent, for conjugated fasudil at 100 µmolar did not yield significance against the group LPA-Met; (3) given that significant differences appeared both in groups treated with CC and without it, it can be stated that, when RHO/ROCK is activated, AMPK activation does not interfere with the GAP43 expression increase fostered by fasudil.

On whether RHO/ROCK signaling may exert a direct effect on GAP43, some words can be said. At this respect, regarding what is known about the regulation of GAP43 activity, it is dependent on Ca^{2+} levels and phosphorylation by PKC (Protein Kinase C). GAP43 presents two binding sites for CaM

A

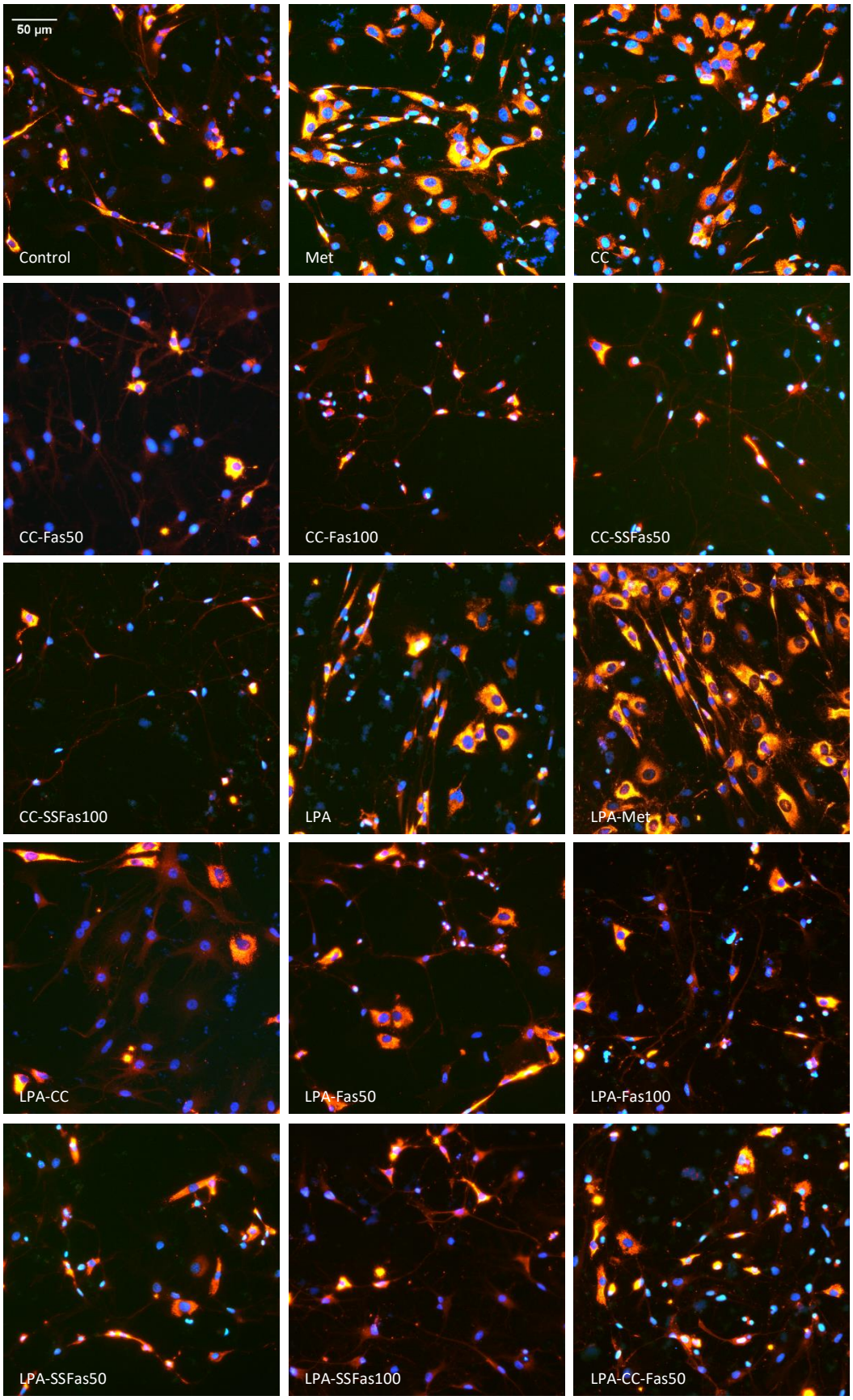
50 µm
Control
Met
CC
CC-Fas50
CC-Fas100
CC-SSFas50
CC-SSFas100
LPA
LPA-Met
LPA-CC
LPA-Fas50
LPA-Fas100
LPA-SSFas50
LPA-SSFas100
LPA-CC-Fas50

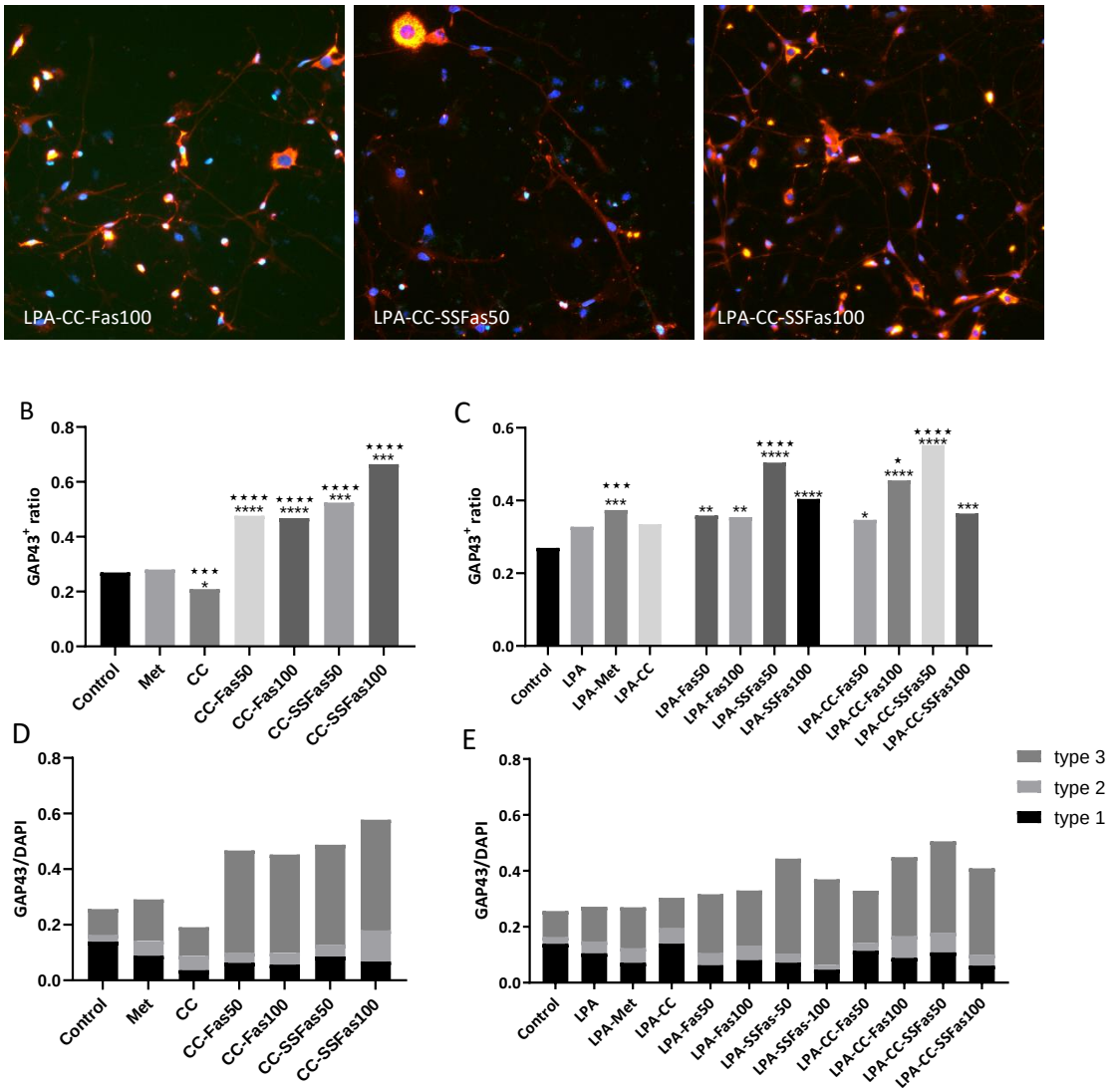

Figure 11. Change in GAP43 expression. (A) Snapshots of cell subject of the different treatments. **(B)** Fold change in proportion of cells presenting GAP43⁺ neurites in treatments without LPA**. (C)** Fold change in proportion of cells presenting GAP43⁺ neurites in treatments with LPA**. (D)** Contribution of type 1, 2 and 3 cells to the total population in cells treated without LPA. **(E).** Contribution of type 1, 2 and 3 cells to the total population in cells treated with LPA. LPA: lysophosphatidic acid, Met: Metformin, CC: Compound C, Fas50: Fasudil at 50 µmolar, Fas100: Fasudil at 100 µmolar, SSFas50: conjugated fasudil at 50 µmolar, SSFas100: conjugated fasudil at 100 µmolar. (* significance against control;* significance against Met or LPA-Met; p-value <0.01 *, p-value<0.001 **, p-value <0.0001 ***, p-value<0.00001 ****, α=0.01).

(calmodulin) and for PKC. When Ca^{2+} levels are low, CaM is bound to GAP43 and inhibits its phosphorylation by PKC. When Ca^{2+} increases, CaM is released and this allows PKC-driven GAP43 phosphorylation. At this point, GAP43 can promote axonal growth via several mechanisms: (1) direct neurite outgrowth via interactions with PiP2, (2) vesicle exchange and (3) release of CaM which indirectly activates actin polymerization (Holahan, 2017). Therefore, we cannot establish a direct molecular link between RHO/ROCK and GAP43.

Finally, observing figures **11D, E**, it is seen that the fold change is majorly due to the fact that type 3 cells are present in a higher proportion to the total population. These cells are the ones with a reduced soma and positive for GAP43 in their neurites and they happen to usually exhibit long axons. In fact, mean neurite length for the treatments including fasudil were significantly higher (**Fig. 9**). As such, we encounter that a higher neurite length is supported by a higher presence of GAP43 in

neurites, mostly found in cells with a reduced soma and long GAP43^{+} axonal projections and, importantly, the best results were obtained in the groups treated with conjugated fasudil, providing evidence for its utility.

Compound C exhibits toxicity and this is partially reversed by conjugated fasudil.

To test the toxicity of compound C on epSPCs as well as the different toxicity between the free and conjugated form of the drug, Casp3^{+} cells were quantified in an ICQ assay (**Fig. 12, S. Table1**). As it was known, NAC exerted a protective effect against apoptosis. Every treatment including CC showed a significantly higher proportion of apoptotic cells as compared to control. Notably, as opposed to previous results showing fasudil as a protective agent, treatments with Fas50 and SSFas100 showed a significantly higher proportion of apoptotic cells as compared to control. Anyway, treatments with fasudil alone (either free or conjugated and not including CC) did show a significantly lower ratio than the CC group, which supports the protective action of the compound. When both compound c and fasudil were combined, only those including the conjugate form showed a significantly lower Casp3^{+} proportion as when compared to the CC group. Summing up, compound C exerted a toxic effect on epSPCs cells; fasudil, free or conjugated, also showed toxicity in two cases, but in a lower extent than CC; and conjugated fasudil was able to revert to a certain extent the toxicity of compound C.

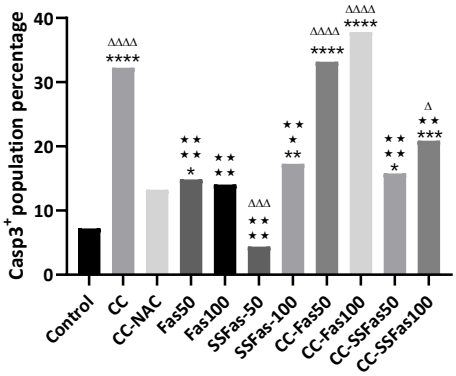

Figure 12. Casp3+ cells referred to DAPI for treatments with fasudil and CC. All the treatments with fasudil include also NAC.CC: Compound C, Fas50: Fasudil at 50 µmolar, Fas100: Fasudil at 100 µmolar, SSFas50: conjugated fasudil at 50 µmolar, SSFas100: conjugated fasudil at 100 µmolar, NAC: N-acetyl-cysteine. (* significance against control, * significance against CC, only tested for treatments having both CC and fasudil; Δ significance against CC-NAC; p-value <0.05 *, p-value<0.01 **, p-value <0.001 ***, p-value<0.0001 ****; α=0.05) .

Gathering the information from these three molecular markers, nestin, GAP43 and Casp3, we can conclude in relation with the objectives of the present project that (1) AMPK seems not to be involved in the ROCK-inhibition dependent enhancement of neurite outgrowth driven by fasudil and (2) the conjugated form of the drug shows a better performance, both in promoting growth of neural processes(neurite length supported by GAP43 build-up) and in the antiapoptotic activity.

Molecular biology

Three have been the objectives of the molecular biology in the *in vitro* experiments:

- Assess the activation/inhibition of Rho/ROCK upon Fasudil/LPA addition.
- Assess the activation/inhibition of AMPK upon Met/CC addition
- Analyze signals of apoptosis and autophagy activation.

The analyses of apoptosis and autophagy are due to the links that have been found between Rho/ROCK and AMPK with these processes, and the involvement of them in axonal regeneration. At this regard, there is accumulative evidence that Rho/Rock pathway activation leads to apoptosis (Koch et al., 2018). Activation of Rho/ROCK signaling in neural cells has been associated to induction

of apoptosis via activation of PTEN and inhibition of Akt. In the same direction, inhibition of Rho/ROCK has shown to inhibit apoptosis associated with upregulation of Akt and inhibition of PTEN (Wu et al., 2012). One of the actions that Rho/ROCK promotes in apoptotic cells is membrane blebbing via phosphorylation of myosin light chain (Mills et al., 1998). ROCK could also promote apoptosis via phosphorylation of ezrin, which leads to activation of Fas (Piazzolla et al., 2005). Hébert et al., (2008) postulate that aggregation of Fas requires the presence of phosphorylated ezrin-moesin complexes, and that this phosphorylation is driven by ROCK. Therefore, inhibition of either Rho or ROCK prevents ezrin and moesin phosphorylation thereby avoiding the early steps of apoptosis. However, which is the link between PTEN/Akt and apoptosis? ROCK phosphorylates PTEN, which becomes active and acts as a negative regulator of the PI3K/Akt pathway. Akt is associated to cell survival, "possibly through inhibition of both the extrinsic and the intrinsic pathways", according to (Shi and Wei, 2007).

Considering the influence of Rho/ROCK in autophagy, downregulation of RHO/ROCK pathway enhances this process (Koch et al., 2018). In particular, this has been proven with fasudil-mediated ROCK inhibition (Liu et al., 2016), although this research is related with neural damage due to α-synuclein, not to a traumatic event. Iorio et al., (2010) also refer that Fasudil does enhance autophagy, and Kitaoka et al., (2017) showed that ripasudil, another ROCK inhibitor, impeded axonal degeneration via activation of autophagy in a model of optic nerve lesion. Indeed, in most cell types and conditions examined, ROCK suppresses autophagy and ROCK-inhibition promotes it.

Regarding the role of AMPK in apoptosis, metformin, an AMPK molecular agonist, (Rena, Hardie, & Pearson 2017) has provided protection against apoptosis in primary cortical neurons *in vitro*(El-Mir et al., 2008, Jiang et al., 2014). In relation to autophagy, AMPK and mTOR regulate this process via phosphorylation of Ulk1 (Kim et al., 2011). Whereas AMPK-mediated phosphorylation promotes autophagy, mTOR-mediated phosphorylation suppresses it. Briefly, AMPK-driven phosphorylation of Ulk1 at Ser317 and Ser777 activates it and induces autophagy. On the other hand, mTOR phosphorylates Ulk1 at Ser757, disrupting the interaction between Ulk1 and AMPK. Additionally, AMPK inhibits mTORC1 (mTOR complex 1) via activation of TSC2 (an mTOR inhibitor). This reduces phosphorylation of Ser757, allowing complex formation with AMPK and Ulk1 activation. Finally, as said in the introduction, autophagy has been associated to axon growth (Clarke and Mearow 2016, Wang et al. 2018), also in the context of SCI (He et al., 2016).

Taking these into account and what was said in the introduction, the direct individual changes that are expected upon treatment with specific compounds are:

- Metformin: as an activator of AMPK, increase in the ratio pAMPK/AMPK, increase in autophagy markers (LCRB and Beclin1) and decrease in pMTOR.
- Compound C: as an inhibitor of AMPK, decrease in the ratio pAMPK/AMPK, decrease in autophagy markers (LCRB and Beclin1) and decrease in pMTOR.
- Fasudil: as an inhibitor of ROCK, decrease in pMYPT, decrease in Casp3, increase in mTOR, and therefore, increase in pCREB and decrease in autophagy markers LC3B and Beclin1
- LPA: as an activator, increase in pMYPT, increase in Casp3, decrease in mTOR and therefore, decrease in pCREB and increase in autophagy markers LC3B and Beclin1.

The experiments were performed, and results are presented (**Fig. 12** and **Fig. 13**), but these results are not reliable due to (1) the fact that the loading control is not valid and (2) that in some occasions the membrane was scrapped or badly marked with the ECL reagent, as it occurred for pCREB (**Fig. 12B**). Because of this I will only give some hints about these results and not talk about the possible differences between treatments with the free and conjugated form of fasudil.

On the inactivation of Rho/ROCk by fasudil, results are not consistent, for samples from cells treated with fasudil show a higher pMYPT expression (**Fig.12 A**). About AMPK activation, cells treated with metformin have shown an increased pAMPK/AMPK ratio as compared with those treated with CC (both when LPA was absent and present) (**Fig. 13A**). Interestingly, treatments with fasudil, either free or conjugated, at 50 µmolar presented a higher pAMPK/AMPK ratio compared to treatments at 100 µmolar. In concomitance with this observation, the autophagy-related LC3B and Beclin1 proteins also showed a higher expression in treatments with fasudil at 50 µmolar (**Fig. 12 D, E**), which would support the fact that fasudil may activate AMPK and this activation enhances autophagy. However,

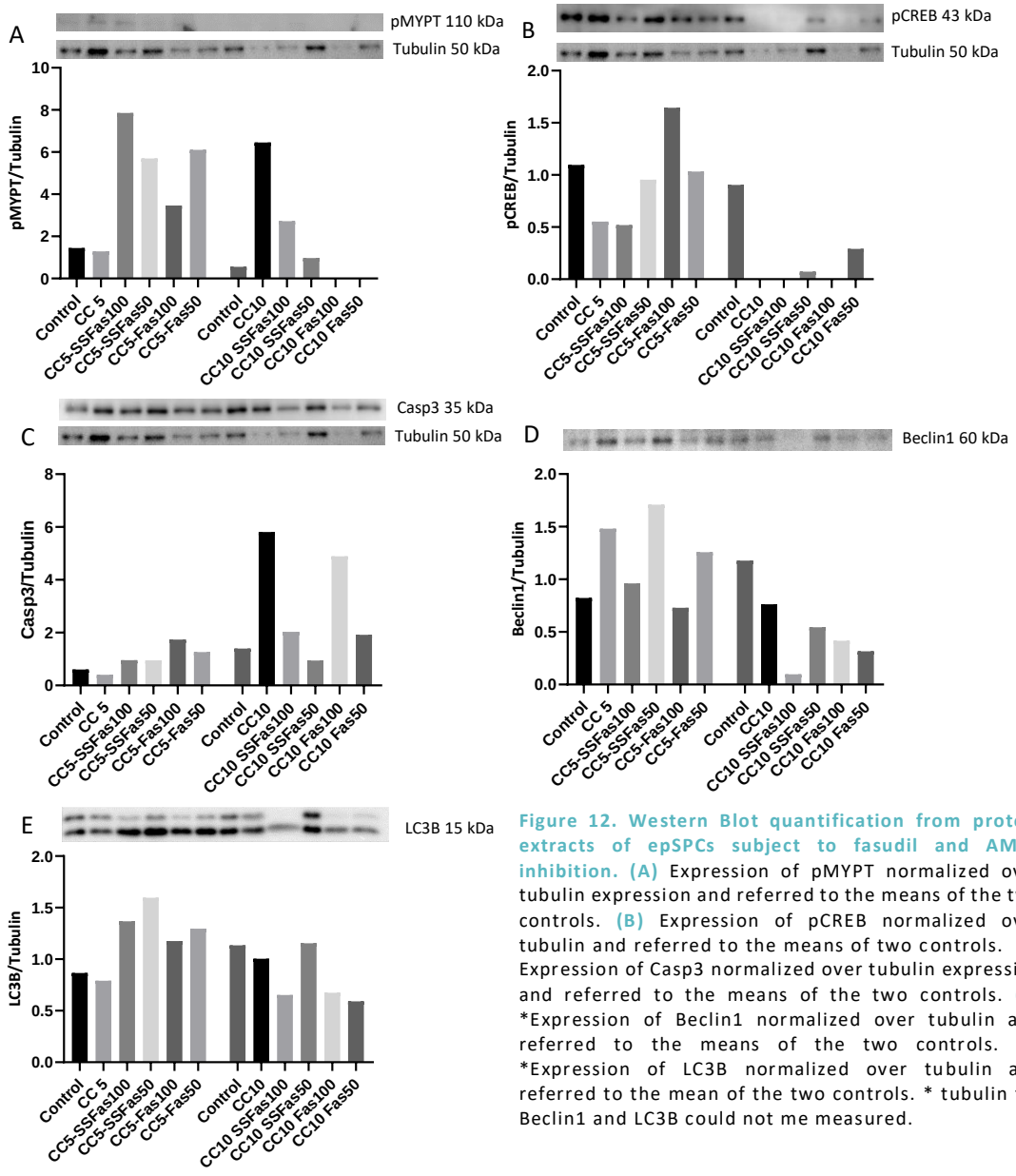

Figure 12. Western Blot quantification from protein extracts of epSPCs subject to fasudil and AMPK inhibition. (A) Expression of pMYPT normalized over tubulin expression and referred to the means of the two controls. **(B)** Expression of pCREB normalized over tubulin and referred to the means of two controls. **(C)** Expression of Casp3 normalized over tubulin expression and referred to the means of the two controls. **(D)** *Expression of Beclin1 normalized over tubulin and referred to the means of the two controls. **(E)** *Expression of LC3B normalized over tubulin and referred to the mean of the two controls. * tubulin for Beclin1 and LC3B could not me measured.

the expression of these two proteins could not be normalized to any load control. Finally, for the apoptosis marker Casp3, there seems not to have been any noticeable fasudil-driven antiapoptotic effect.

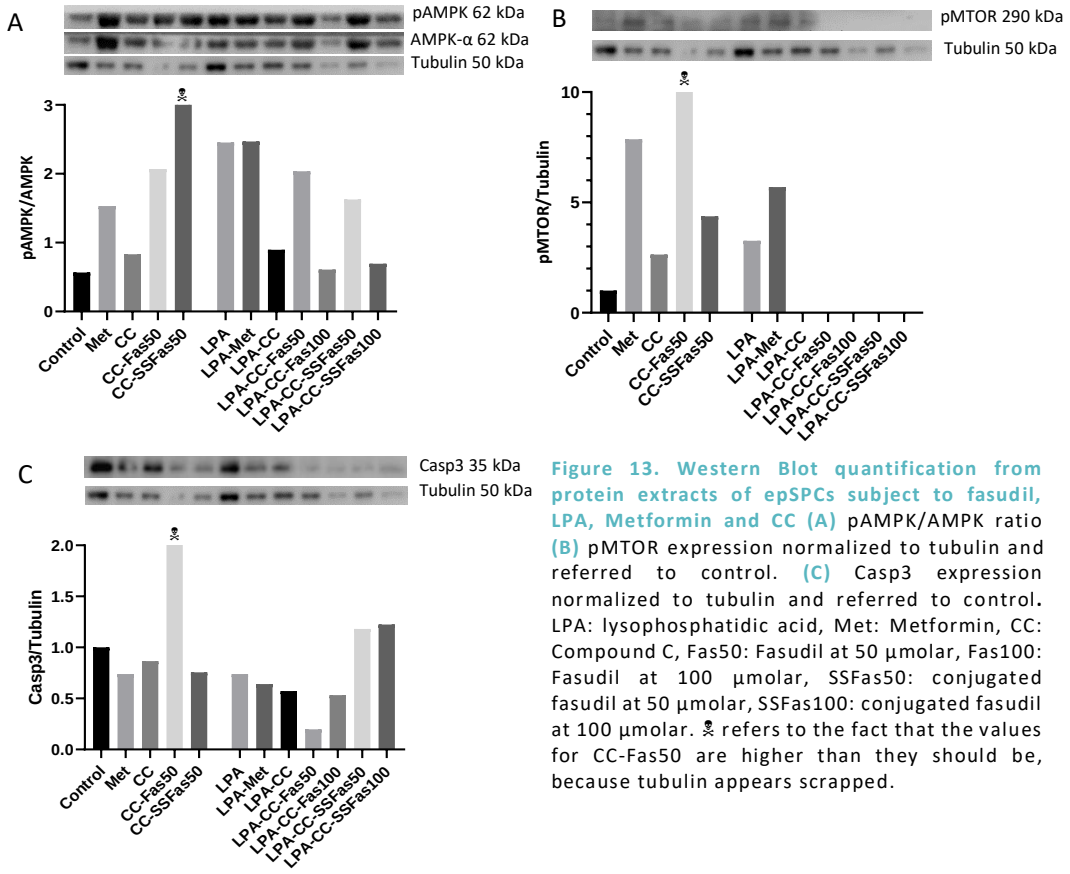

Figure 13. Western Blot quantification from protein extracts of epSPCs subject to fasudil, LPA, Metformin and CC (A) pAMPK/AMPK ratio **(B)** pMTOR expression normalized to tubulin and referred to control. **(C)** Casp3 expression normalized to tubulin and referred to control. LPA: lysophosphatidic acid, Met: Metformin, CC: Compound C, Fas50: Fasudil at 50 µmolar, Fas100: Fasudil at 100 µmolar, SSFas50: conjugated fasudil at 50 µmolar, SSFas100: conjugated fasudil at 100 µmolar. ☠ refers to the fact that the values for CC-Fas50 are higher than they should be, because tubulin appears scrapped.

V. CONCLUSION.

Many efforts have been put in different directions to regenerate the neural tissue in the spinal cord. In this day and age, cell therapy appears as one of the one of the horses that is getting the highest bets, provided evidence gathered so far and their adaptability and versatility to exert a modulating influence on the lesion microenvironment and yet, there is still room for improvement of pharmacological treatments.

In this way, the Neuronal and Tissue Regeneration group at the CIPF has been focusing part of its effort in the development of a cell therapy for SCI involving epSPCs and the conjugation of the known ROCK inhibitor fasudil so as to improve its efficacy as a proven axonal growth stimulating agent. An *in vivo* assay in *Rattus norvegicus* was lanced and its analysis is still ongoing. As far as this project is concerned, the histological analysis performed has shown not to yield signs of improvement: extension of tissue degeneration was even among treatments, there was not a different, conservation of motor neurons, even if significant differences were found for the extension of the glial scar, the cause of this is elusive; and axonal tract conservation required a more precise analysis. However, it was conjugated fasudil that showed the most efficient inhibition of RHO/ROCK, as shown by the WB results. This may be the sign of a lower degradability and a better performance, given the fact that the direct primary effect of the drug fasudil is the disruption of this signaling pathway.

The similar results obtained among the distinct treatments may be simply due to the fact that we were dealing with a chronic model, in which the secondary damage has taken place and the scarring process has been stabilized and assented. In any case, more analysis are awaiting (oligodendrocyte population, synapse activity, survival and migration of transplanted cells…) that will better characterize the state of the spinal cord in these animals, although, in order to be able to do a more thorough analysis, efforts should directed towards the application of other techniques for axonal visualization.

On the observation that fasudil administration was followed by a peak on AMPK activity, the group came interested in testing whether compromising the activation of AMPK would also compromise the axonal growth enhancement driven by fasudil. *In vitro* assays on epSPCs carried out in this project have shown that this is not the case.

Finally, *in vitro* assays also threw evidence that the developed PGA-SSFasudil conjugated form of the is preferable to achieve neurite outgrowth in epSPCs, since treatments with conjugated fasudil yielded the best results for neurite length, for the expression of the axonal growth associated GAP43 and for antiapoptotic event. Of note, an apparent dose-effect appeared, and therefore it would be convenable to better test this phenomenon. Unfortunately, not trustworthy information could be drawn from the WB experiments, but ICQ results are promising.

As more steps are taken for the continuous improvement of cellular and pharmacological approaches, together with the electric-stimulatory strategies followed by other groups and the recent cutting-edge technologies for tissue visualization, advances are being made towards the eventual functional regeneration of the injured spinal cord, and, albeit cautious, we must be optimistic about the years to come.

VI. REFERENCES.

ABE, N.; BORSON, S.H.; GAMBELLO, M.J.; WANG, F. & CAVALLI, V. (2010). Mammalian target of rapamycin (mTOR) activation increases axonal growth capacity of injured peripheral nerves. *J. Biol. Chem*. 285, 28034–43. https://doi.org/10.1074/jbc.M110.125336

AGHANOORI, M.-R.; SMITH, D.R.; SHARIATI-IEVARI, S.; AJISEBUTU, A.; NGUYEN, A.; DESMOND, F.; JESUS, C.H.A.; ZHOU, X.; CALCUTT, N.A.; ALIANI, M. & FERNYHOUGH, P. (2019). Insulin-like growth factor-1 activates AMPK to augment mitochondrial function and correct neuronal metabolism in sensory neurons in type 1 diabetes. *Mol. Metab*. 20, 149–165. https://doi.org/10.1016/J.MOLMET.2018.11.008

ANDERSON, M.A.; BURDA, J.E.; REN, Y.; AO, Y.; O'SHEA, T.M.; KAWAGUCHI, R.; COPPOLA, G.; KHAKH, B.S.; DEMING, T.J. & SOFRONIEW, M. V. (2016). Astrocyte scar formation aids central nervous system axon regeneration. *Nature* 532, 195–200. https://doi.org/10.1038/nature17623

ASSINCK, P.; DUNCAN, G.J.; HILTON, B.J.; PLEMEL, J.R. & TETZLAFF, W. (2017). Cell transplantation therapy for spinal cord injury. *Nat. Neurosci*. 20, 637–647. https://doi.org/10.1038/nn.4541

BARBER, R.P.; PHELPS, P.E.; HOUSER, C.R.; CRAWFORD, G.D.; SALVATERRA, P.M. & VAUGHN, J.E. (1984). The morphology and distribution of neurons containing choline acetyltransferase in the adult rat spinal cord: An immunocytochemical study. *J. Comp. Neurol.* 229, 329–346. https://doi.org/10.1002/cne.902290305

BARDEHLE, S.; KRÜGER, M.; BUGGENTHIN, F.; SCHWAUSCH, J.; NINKOVIC, J.; CLEVERS, H.; SNIPPERT, H.J.; THEIS, F.J.; MEYER-LUEHMANN, M.; BECHMANN, I.; DIMOU & L. & GÖTZ, M. (2013). Live imaging of astrocyte responses to acute injury reveals selective juxtavascular proliferation. *Nat. Neurosci*. 16, 580–586. https://doi.org/10.1038/nn.3371

BAREYRE, F.M.; KERSCHENSTEINER, M.; MISGELD, T. & SANES, J.R. (2005). Transgenic labeling of the corticospinal tract for monitoring axonal responses to spinal cord injury. *Nat. Med*. 11, 1355–1360. https://doi.org/10.1038/nm1331

BARNABÉ-HEIDER, F.; GÖRITZ, C.; SABELSTRÖM, H.; TAKEBAYASHI, H.; PFRIEGER, F.W.; MELETIS, K. & FRISÉN, J. (2010). Origin of new glial cells in intact and injured adult spinal cord. *Cell Stem Cell* 7, 470–82. https://doi.org/10.1016/j.stem.2010.07.014

BEN-YAAKOV, K.; DAGAN, S.Y.; SEGAL-RUDER, Y.; SHALEM, O.; VUPPALANCHI, D.; WILLIS, D.E.; YUDIN, D.; RISHAL, I.; ROTHER, F.; BADER, M.; BLESCH, A.; PILPEL, Y.; TWISS, J.L. & FAINZILBER, M. (2012). Axonal transcription factors signal retrogradely in lesioned peripheral nerve. *EMBO J*. 31, 1350–1363. https://doi.org/10.1038/emboj.2011.494

BERRY, M.; AHMED, Z.; MORGAN-WARREN, P.; FULTON, D. & LOGAN, A. (2016). Prospects for mTOR-mediated functional repair after central nervous system trauma. *Neurobiol. Dis*. 85, 99–110. https://doi.org/10.1016/J.NBD.2015.10.002

BOATO, F.; HENDRIX, S.; HUELSENBECK, S.C.; HOFMANN, F.; GROSSE, G.; DJALALI, S.; KLIMASCHEWSKI, L.; AUER, M.; JUST, I.; AHNERT-HILGER, G.& HÖLTJE, M. (2010). C3 peptide enhances recovery from spinal cord injury by improved regenerative growth of descending fiber tracts. *J. Cell Sci*. 123, 1652–62. https://doi.org/10.1242/jcs.066050

BRADKE, F.; FAWCETT, J.W. & SPIRA, M.E. (2012). Assembly of a new growth cone after axotomy: The precursor to axon regeneration. *Nat. Rev. Neurosci.* 13, 183–193. https://doi.org/10.1038/nrn3176

BURDA, J.E. & SOFRONIEW, M. V. (2014). Reactive gliosis and the multicellular response to CNS damage and disease. *Neuron* 81, 229–48. https://doi.org/10.1016/j.neuron.2013.12.034

BUSCH, S.A.; HORN, K.P.; CUASCUT, F.X.; HAWTHORNE, A.L.; BAI, L.; MILLER, R.H. & SILVER, J. (2010). Adult NG2+ cells are permissive to neurite outgrowth and stabilize sensory axons during macrophage-induced axonal dieback after spinal cord injury. *J. Neurosci*. 30, 255–65. https://doi.org/10.1523/JNEUROSCI.3705-09.2010

BUSH, T.G.; PUVANACHANDRA, N.; HORNER, C.H.; POLITO, A.; OSTENFELD, T.; SVENDSEN, C.N.; MUCKE, L.; JOHNSON, M.H. & SOFRONIEW, M. V. (1999). Leukocyte infiltration, neuronal degeneration, and neurite outgrowth after ablation of scar-forming, reactive astrocytes in adult transgenic mice. *Neuron* 23, 297–308. https://doi.org/10.1016/S0896-6273(00)80781-3

CAPOGROSSO, M.; MILEKOVIC, T.; BORTON, D.; WAGNER, F.; MORAUD, E.M.; MIGNARDOT, J.B.; BUSE, N.; GANDAR, J.; BARRAUD, Q.; XING, D.; REY, E.; DUIS, S.; JIANZHONG, Y.; KO, W.K.D.; LI, Q.; DETEMPLE, P.; DENISON, T.; MICERA, S.; BEZARD, E.; BLOCH, J. & COURTINE, G. (2016). A brain-spine interface alleviating gait deficits after spinal cord injury in primates. *Nature* 539, 284–288. https://doi.org/10.1038/nature20118

CARROLL, S.L.; (2009). Wallerian Degeneration & Regeneration. *Encycl. Neurosci*. 485–491.

CHEN, Z.-L.; YU, W.-M. & STRICKLAND, S. (2007). Peripheral Regeneration. *Annu. Rev. Neurosci*. 30, 209–233. https://doi.org/10.1146/annurev.neuro.30.051606.094337

CHO, Y.; SLOUTSKY, R.; NAEGLE, K.M. & CAVALLI, V. (2013). Injury-induced HDAC5 nuclear export is essential for axon regeneration. *Cell* 155, 894–908. https://doi.org/10.1016/j.cell.2013.10.004

CHUNG, K. & DEISSEROTH, K. (2013). CLARITY for mapping the nervous system. *Nat. Methods* 10, 508–513. https://doi.org/10.1038/nmeth.2481

CLARKE, J.-P. & MEAROW, K. (2016). Autophagy inhibition in endogenous and nutrient-deprived conditions reduces dorsal root

ganglia neuron survival and neurite growth in vitro. *J. Neurosci*. Res. 94, 653–670. https://doi.org/10.1002/jnr.23733

COURTINE, G.; SONG, B.; ROY, R.R.; ZHONG, H.; HERRMANN, J.E.; AO, Y.; QI, J.; EDGERTON, V.R.& SOFRONIEW, M. V. (2008). Recovery of supraspinal control of stepping via indirect propriospinal relay connections after spinal cord injury. *Nat. Med*. 14, 69–74. https://doi.org/10.1038/nm1682

DA CUNHA, A.; ALOYO, V.J. & VITKOVIĆ, L. (1991). Developmental regulation of GAP-43, glutamine synthetase and β-actin mRNA in rat cortical astrocytes. *Dev. Brain Res*. 64, 212–215. https://doi.org/10.1016/0165-3806(91)90228-B

DAVID, S. & AGUAYO, A.J. (1981). Axonal elongation into peripheral nervous system "bridges" after central nervous system injury in adult rats. *Science* 214, 931–3. https://doi.org/10.1126/science.6171034

DAVIES, J.E.; HUANG, C.; PROSCHEL, C.; NOBLE, M.; MAYER-PROSCHEL, M. & DAVIES, S.J. (2006). Astrocytes derived from glial-restricted precursors promote spinal cord repair. *J. Biol*. 5, 7. https://doi.org/10.1186/jbiol35

DEPAUL, M.A.; PALMER, M.; LANG, B.T.; CUTRONE, R.; TRAN, A.P.; MADALENA, K.M.; BOGAERTS, A.; HAMILTON, J.A.; DEANS, R.J.; MAYS, R.W.; BUSCH, S.A. & SILVER, J. (2015). Intravenous multipotent adult progenitor cell treatment decreases inflammation leading to functional recovery following spinal cord injury. *Sci. Rep*. 5, 16795. https://doi.org/10.1038/srep16795

DICKENDESHER, T.L.; BALDWIN, K.T.; MIRONOVA, Y.A.; KORIYAMA, Y.; RAIKER, S.J.; ASKEW, K.L.; WOOD, A.; GEOFFROY, C.G.; ZHENG, B.; LIEPMANN, C.D.; KATAGIRI, Y.; BENOWITZ, L.I.; GELLER, H.M. & GIGER, R.J. (2012). NgR1 and NgR3 are receptors for chondroitin sulfate proteoglycans. *Nat. Neurosci*. 15, 703–712. https://doi.org/10.1038/nn.3070

DILL, J.; WANG, H.; ZHOU, F. & LI, S. (2008). Inactivation of glycogen synthase kinase 3 promotes axonal growth and recovery in the CNS. *J. Neurosci.* 28, 8914–28. https://doi.org/10.1523/JNEUROSCI.1178-08.2008

DONNELLY, C.J.; PARK, M.; SPILLANE, M.; YOO, S.; PACHECO, A.; GOMES, C.; VUPPALANCHI, D.; MCDONALD, M.; KIM, H.H.; MERIANDA, T.T.; GALLO, G. & TWISS, J.L. (2013). Axonally Synthesized -Actin and GAP-43 Proteins Support Distinct Modes of Axonal Growth. *J. Neurosci*. 33, 3311–3322. https://doi.org/10.1523/jneurosci.1722-12.2013

DUGAS, J.C.; MANDEMAKERS, W.; ROGERS, M.; IBRAHIM, A.; DANEMAN, R. & BARRES, B.A. (2008). A Novel Purification Method for CNS Projection Neurons Leads to the Identification of Brain Vascular Cells as a Source of Trophic Support for Corticospinal Motor Neurons. *J. Neurosci*. 28, 8294–8305. https://doi.org/10.1523/JNEUROSCI.2010-08.2008

EL-MIR, M.-Y.; DETAILLE, D.; R-VILLANUEVA, G.; DELGADO-ESTEBAN, M.; GUIGAS, B.; ATTIA, S.; FONTAINE, E.; ALMEIDA, A. & LEVERVE, X. (2008). Neuroprotective Role of Antidiabetic Drug Metformin Against Apoptotic Cell Death in Primary Cortical Neurons. *J. Mol. Neurosci*. 34, 77–87. https://doi.org/10.1007/s12031-007-9002-1

EREZ, H.; MALKINSON, G.; PRAGER-KHOUTORSKY, M.; DE ZEEUW, C.I.; HOOGENRAAD, C.C. & SPIRA, M.E. (2007). Formation of microtubule-based traps controls the sorting and concentration of vesicles to restricted sites of regenerating neurons after axotomy. *J. Cell Biol*. 176, 497–507. https://doi.org/10.1083/jcb.200607098

ERTÜRK, A.; HELLAL, F.; ENES, J. & BRADKE, F. (2007). Disorganized microtubules underlie the formation of retraction bulbs and the failure of axonal regeneration. *J. Neurosci.* 27, 9169–80. https://doi.org/10.1523/JNEUROSCI.0612-07.2007

FAULKNER, J.R.; HERRMANN, J.E.; WOO, M.J.; TANSEY, K.E.; DOAN, N.B. & SOFRONIEW, M. V. (2004). Reactive astrocytes protect tissue and preserve function after spinal cord injury. *J. Neurosci.* 24, 2143–55. https://doi.org/10.1523/JNEUROSCI.3547-03.2004

FILOUS, A.R. & SILVER, J. (2016). "Targeting astrocytes in CNS injury and disease: A translational research approach." *Prog. Neurobiol.* 144, 173–187. https://doi.org/10.1016/J.PNEUROBIO.2016.03.009

FRANCOS-QUIJORNA, I.; AMO-APARICIO, J.; MARTINEZ-MURIANA, A. & LÓPEZ-VALES, R. (2016). IL-4 drives microglia and macrophages toward a phenotype conducive for tissue repair and functional recovery after spinal cord injury. *Glia* 64, 2079–2092. https://doi.org/10.1002/glia.23041

FRANKLIN, R.J.M. & FFRENCH-CONSTANT, C. (2008). Remyelination in the CNS: from biology to therapy. *Nat. Rev. Neurosci*. 9, 839–855. https://doi.org/10.1038/nrn2480

FUJITA, Y. & YAMASHITA, T. (2014). Axon growth inhibition by RhoA/ROCK in the central nervous system. *Front. Neurosci.* 8, 1–12. https://doi.org/10.3389/fnins.2014.00338

GAO, Y.; DENG, K.; HOU, J.; BRYSON, J.B.; BARCO, A.; NIKULINA, E.; SPENCER, T.; MELLADO, W.; KANDEL, E.R. & FILBIN, M.T. (2004). Activated CREB is sufficient to overcome inhibitors in myelin and promote spinal axon regeneration in vivo. *Neuron* 44, 609–21. https://doi.org/10.1016/j.neuron.2004.10.030

GÖRITZ, C.; DIAS, D.O.; TOMILIN, N.; BARBACID, M.; SHUPLIAKOV, O. & FRISÉN, J. (2011). A pericyte origin of spinal cord scar tissue. *Science* 333, 238–42. https://doi.org/10.1126/science.1203165

GRASSNER, L.; MARSCHALLINGER, J.; DÜNSER, M.W.; NOVAK, H.F.; ZERBS, A.; AIGNER, L.; TRINKA, E. & SELLNER, J. (2016). Nontraumatic spinal cord injury at the neurological intensive care unit: Spectrum, causes of admission and predictors of mortality. *Ther. Adv. Neurol. Disord*. 9, 85–94. https://doi.org/10.1177/1756285615621687

GUSEL'NIKOVA, V. & KORZHEVSKIY, D.E. (2015). NeuN As a Neuronal Nuclear Antigen and Neuron Differentiation Marker. *Acta Naturae* 7, 42–7.

HAGEN, E.M. (2015). Acute complications of spinal cord injuries. *World J. Orthop*. 6, 17. https://doi.org/10.5312/wjo.v6.i1.17

HAO, Y.; FREY, E.; YOON, C.; WONG, H.; NESTOROVSKI, D.; HOLZMAN, L.B.; GIGER, R.J.; DIANTONIO, A. & COLLINS, C. (2016). An evolutionarily conserved mechanism for cAMP elicited axonal regeneration involves direct activation of the dual leucine zipper kinase DLK. *Elife 5*. https://doi.org/10.7554/eLife.14048

HE, M.; DING, Y.; CHU, C.; TANG, J.; XIAO, Q. & LUO, Z.-G. (2016). Autophagy induction stabilizes microtubules and promotes axon regeneration after spinal cord injury. *Proc. Natl. Acad. Sci. U. S. A.* 113, 11324–11329. https://doi.org/10.1073/pnas.1611282113

HE, Z. & JIN, Y. (2016). Intrinsic Control of Axon Regeneration. *Neuron* 90, 437–451. https://doi.org/10.1016/J.NEURON.2016.04.022

HÉBERT, M.; POTIN, S.; SEBBAGH, M.; BERTOGLIO, J.; BRÉARD, J. & HAMELIN, J. (2008). Rho-ROCK-Dependent Ezrin-Radixin-Moesin Phosphorylation Regulates Fas-Mediated Apoptosis in Jurkat Cells. *J. Immunol.* 181, 5963–5973. https://doi.org/10.4049/JIMMUNOL.181.9.5963

HERMANNS, S.; KLAPKA, N.; GASIS, M. & MÜLLER, H.W. (2006). The Collagenous Wound Healing Scar in the Injured Central Nervous System Inhibits Axonal Regeneration, in: *Brain Repair. Springer US, Boston, MA,* pp. 177–190. https://doi.org/10.1007/0-387-30128-3_11

HOLAHAN, M. (2015). GAP-43 in synaptic plasticity: molecular perspectives. *Res. Reports Biochem.* 5, 137. https://doi.org/10.2147/RRBC.S73846

HOLAHAN, M.R. (2017). A Shift from a Pivotal to Supporting Role for the Growth-Associated Protein (GAP-43) in the Coordination of Axonal Structural and Functional Plasticity. *Front. Cell. Neurosci*. 11, 266. https://doi.org/10.3389/fncel.2017.00266

HOULE, J.D. (1991). Demonstration of the potential for chronically injured neurons to regenerate axons into intraspinal peripheral nerve grafts. *Exp. Neurol.* 113, 1–9. https://doi.org/10.1016/0014-4886(91)90139-4

IORIO, F.; BOSOTTI, R.; SCACHERI, E.; BELCASTRO, V.; MITHBAOKAR, P.; FERRIERO, R.; MURINO, L.; TAGLIAFERRI, R.; BRUNETTI-PIERRI, N.; ISACCHI, A. & DI BERNARDO, D. (2010). Discovery of drug mode of action and drug repositioning from transcriptional responses. *Proc. Natl. Acad. Sci. U. S. A.* 107, 14621–6. https://doi.org/10.1073/pnas.1000138107

ISHIZUKA, Y.; KAKIYA, N.; WITTERS, L.A.; OSHIRO, N.; SHIRAO, T.; NAWA, H. & TAKEI, N. (2013). AMP-activated protein kinase counteracts brain-derived neurotrophic factor-induced mammalian target of rapamycin complex 1 signaling in neurons. *J. Neurochem*. 127, n/a-n/a. https://doi.org/10.1111/jnc.12362

JALINK, K.; VAN CORVEN, E.J.; HENGEVELD, T.; MORII, N.; NARUMIYA, S. & MOOLENAAR, W.H. (1994). Inhibition of lysophosphatidate- and thrombin-induced neurite retraction and neuronal cell rounding by ADP ribosylation of the small GTP-binding protein Rho. *J. Cell Biol*. 126, 801–10. https://doi.org/10.1083/jcb.126.3.801

JIANG, T.; YU, J.-T.; ZHU, X.-C.; WANG, H.-F.; TAN, M.-S.; CAO, L.; ZHANG, Q.-Q.; GAO, L.; SHI, J.-Q.; ZHANG, Y.-D. & TAN, L. (2014). Acute metformin preconditioning confers neuroprotection against focal cerebral ischaemia by pre-activation of AMPK-dependent autophagy. *Br. J. Pharmacol*. 171, 3146–3157. https://doi.org/10.1111/bph.12655

JIN, Y.; FISCHER, I.; TESSLER, A. & HOULE, J.D. (2002). Transplants of Fibroblasts Genetically Modified to Express BDNF Promote Axonal Regeneration from Supraspinal Neurons Following Chronic Spinal Cord Injury. *Exp. Neurol*. 177, 265–275. https://doi.org/10.1006/EXNR.2002.7980

JOHANSSON, C.B.; MOMMA, S.; CLARKE, D.L.; RISLING, M.; LENDAHL, U. & FRISÉN, J. (1999). Identification of a neural stem cell in the adult mammalian central nervous system. *Cell* 96, 25–34. https://doi.org/10.1016/S0092-8674(00)80956-3

KADOYA, K.; LU, P.; NGUYEN, K.; LEE-KUBLI, C.; KUMAMARU, H.; YAO, L.; KNACKERT, J.; POPLAWSKI, G.; DULIN, J.N.; STROBL, H.; TAKASHIMA, Y.; BIANE, J.; CONNER, J.; ZHANG, S.-C. & TUSZYNSKI, M.H. (2016). Spinal cord reconstitution with homologous neural grafts enables robust corticospinal regeneration. *Nat. Med.* 22, 479–487. https://doi.org/10.1038/nm.4066

KEIRSTEAD, H.S.; NISTOR, G.; BERNAL, G.; TOTOIU, M.; CLOUTIER, F.; SHARP, K. & STEWARD, O. (2005). Human Embryonic Stem Cell-Derived Oligodendrocyte Progenitor Cell Transplants Remyelinate and Restore Locomotion after Spinal Cord Injury. *J. Neurosci.* 25, 4694–4705. https://doi.org/10.1523/JNEUROSCI.0311-05.2005

KIGERL, K.A.; GENSEL, J.C.; ANKENY, D.P.; ALEXANDER, J.K.; DONNELLY, D.J. & POPOVICH, P.G. (2009). Identification of two distinct macrophage subsets with divergent effects causing either neurotoxicity or regeneration in the injured mouse spinal cord. *J. Neurosci.* 29, 13435–44. https://doi.org/10.1523/JNEUROSCI.3257-09.2009

KIM, J.; KUNDU, M.; VIOLLET, B. & GUAN, K.-L. (2011). AMPK and mTOR regulate autophagy through direct phosphorylation of Ulk1. *Nat. Cell Biol*. 13, 132–141. https://doi.org/10.1038/ncb2152

KIMURA-KURODA, J.; TENG, X.; KOMUTA, Y.; YOSHIOKA, N.; SANGO, K.; KAWAMURA, K.; RAISMAN, G. & KAWANO, H. (2010). An in vitro model of the inhibition of axon growth in the lesion scar formed after central nervous system injury. *Mol. Cell. Neurosci*. 43, 177–187. https://doi.org/10.1016/J.MCN.2009.10.008

KITAOKA, Y.; SASE, K.; TSUKAHARA, C.; KOJIMA, K.; SHIONO, A.; KOGO, J.; TOKUDA, N. & TAKAGI, H. (2017). Axonal Protection by Ripasudil, a Rho Kinase Inhibitor, via Modulating Autophagy in TNF-Induced Optic Nerve Degeneration. *Investig. Opthalmology Vis. Sci.* 58, 5056. https://doi.org/10.1167/iovs.17-22000

KOCH, J.C.; TATENHORST, L.; ROSER, A.E.; SAAL, K.A.; TÖNGES, L. & LINGOR, P. (2018). ROCK inhibition in models of neurodegeneration and its potential for clinical translation. *Pharmacol. Ther.* 189, 1–21. https://doi.org/10.1016/j.pharmthera.2018.03.008

KRANENBURG, O.; POLAND, M.; VAN HORCK, F.P.G.; DRECHSEL, D.; HALL, A. & MOOLENAAR, W.H. (1999). Activation of RhoA by Lysophosphatidic Acid and Gα $_{12/13}$ Subunits in Neuronal Cells: Induction of Neurite Retraction. *Mol. Biol. Cell* 10, 1851–1857. https://doi.org/10.1091/mbc.10.6.1851

LACROIX, S.; HAMILTON, L.K.; VAUGEOIS, A.; BEAUDOIN, S.; BREAULT-DUGAS, C.; PINEAU, I.; LÉVESQUE, S.A.; GRÉGOIRE, C.-A. & FERNANDES, K.J.L. (2014). Central Canal Ependymal Cells Proliferate Extensively in Response to Traumatic Spinal Cord Injury but Not Demyelinating Lesions. *PLoS One 9*, e85916. https://doi.org/10.1371/journal.pone.0085916

LAUX, T.; FUKAMI, K.; THELEN, M.; GOLUB, T.; FREY, D. & CARONI, P. (2000). Gap43, Marcks, and Cap23 Modulate Pi(4,5)p2 at Plasmalemmal Rafts, and Regulate Cell Cortex Actin Dynamics through a Common Mechanism. *J. Cell Biol*. 149, 1455–1472. https://doi.org/10.1083/JCB.149.7.1455

LEE, B.B.; CRIPPS, R.A.; FITZHARRIS, M. & WING, P.C. (2014). The global map for traumatic spinal cord injury epidemiology: update 2011, global incidence rate. *Spinal Cord* 52, 110–116. https://doi.org/10.1038/sc.2012.158

LEIN, P.J.; BANKER, G.A. & HIGGINS, D. (1992). Laminin selectively enhances axonal growth and accelerates the development of polarity by hippocampal neurons in culture. *Dev. Brain Res*. 69, 191–197. https://doi.org/10.1016/0165-3806(92)90159-T

LI, Y.; FIELD, P.M. & RAISMAN, G. (1999). Death of oligodendrocytes and microglial phagocytosis of myelin precede immigration of Schwann cells into the spinal cord. *J. Neurocytol*. 28, 417–427. https://doi.org/10.1023/A:1007026001189

LIN, C.-H.; CHENG, Y.-C.; NICOL, C.J.; LIN, K.-H.; YEN, C.-H. & CHIANG, M.-C. (2017). Activation of AMPK is neuroprotective in the oxidative stress by advanced glycosylation end products in human neural stem cells. *Exp. Cell Res*. 359, 367–373. https://doi.org/10.1016/J.YEXCR.2017.08.019

LIU, F.-T.; YANG, Y.-J.; WU, J.-J.; LI, S.; TANG, Y.-L.; ZHAO, J.; LIU, Z.-Y.; XIAO, B.-G.; ZUO, J.; LIU, W. & WANG, J. (2016). Fasudil, a Rho kinase inhibitor, promotes the autophagic degradation of A53T α-synuclein by activating the JNK 1/Bcl-2/beclin 1 pathway. *Brain Res*. 1632, 9–18. https://doi.org/10.1016/J.BRAINRES.2015.12.002

LIU, K.; LU, Y.; LEE, J.K.; SAMARA, R.; WILLENBERG, R.; SEARS-KRAXBERGER, I.; TEDESCHI, A.; PARK, K.K.; JIN, D.; CAI, B.; XU, B.; CONNOLLY, L.; STEWARD, O.; ZHENG, B. & HE, Z. (2010). PTEN deletion enhances the regenerative ability of adult corticospinal neurons. *Nat. Neurosci*. 13, 1075–1081. https://doi.org/10.1038/nn.2603

LIU, K.; TEDESCHI, A.; KYUNGSUK PARK, K. & HE, Z. (2011). Neuronal Intrinsic Mechanisms of Axon Regeneration. *Annu. Rev. Neurosci*. https://doi.org/10.1038/s41583-018-0001-8

LIU, P.-Y.& LIAO, J.K. (2008). A method for measuring Rho kinase activity in tissues and cells. *Methods Enzymol*. 439, 181–9. https://doi.org/10.1016/S0076-6879(07)00414-4

LOH, Y.-H.E.; KOEMETER-COX, A.; FINELLI, M.J.; SHEN, L.; FRIEDEL, R.H. & ZOU, H. (2017). Comprehensive mapping of 5-hydroxymethylcytosine epigenetic dynamics in axon regeneration. *Epigenetics* 12, 77–92. https://doi.org/10.1080/15592294.2016.1264560

LONDON, A.; COHEN, M. & SCHWARTZ, M. (2013). Microglia and monocyte-derived macrophages: functionally distinct populations that act in concert in CNS plasticity and repair. *Front. Cell. Neurosci*. 7, 34. https://doi.org/10.3389/fncel.2013.00034

LU, P.; JONES, L.L. & TUSZYNSKI, M.H. (2007). Axon regeneration through scars and into sites of chronic spinal cord injury. *Exp. Neurol*. 203, 8–21. https://doi.org/10.1016/J.EXPNEUROL.2006.07.030

LU, P.; WANG, Y.; GRAHAM, L.; MCHALE, K.; GAO, M.; WU, D.; BROCK, J.; BLESCH, A.; ROSENZWEIG, E.S.; HAVTON, L.A.; ZHENG, B.; CONNER, J.M.; MARSALA, M. & TUSZYNSKI, M.H. (2012). Long-distance growth and connectivity of neural stem cells after severe spinal cord injury. *Cell* 150, 1264–73. https://doi.org/10.1016/j.cell.2012.08.020

LUKOVIC, D.; STOJKOVIC, M.; MORENO-MANZANO, V.; JENDELOVA, P.; SYKOVA, E.; BHATTACHARYA, S.S. & ERCEG, S. (2014). Reactive Astrocytes and Stem Cells in Spinal Cord Injury : Good Guys or Bad Guys ? 1–9. *Stem Cells* 33 (4), 1036-1041 https://doi.org/10.1002/stem.1959

MAHAR, M. & CAVALLI, V. (2018). Intrinsic mechanisms of neuronal axon regeneration. *Nat. Rev. Neurosci*. 19, 323–337. https://doi.org/10.1038/s41583-018-0001-8

MCTIGUE, D.M.; WEI, P. & STOKES, B.T. (2001). Proliferation of NG2-positive cells and altered oligodendrocyte numbers in the contused rat spinal cord. *J. Neurosci*. 21, 3392–400. https://doi.org/10.1523/JNEUROSCI.21-10-03392.2001

MELETIS, K.; BARNABÉ-HEIDER, F.; CARLÉN, M.; EVERGREN, E.; TOMILIN, N.; SHUPLIAKOV, O. & FRISÉN, J. (2008a). Spinal Cord Injury Reveals Multilineage Differentiation of Ependymal Cells. *PLoS Biol. 6*, e182. https://doi.org/10.1371/journal.pbio.0060182

MELETIS, K.; BARNABÉ-HEIDER, F.; CARLÉN, M.; EVERGREN, E.; TOMILIN, N.; SHUPLIAKOV, O. & FRISÉN, J. (2008b). Spinal Cord Injury Reveals Multilineage Differentiation of Ependymal Cells. *PLoS Biol. 6*, e182. https://doi.org/10.1371/journal.pbio.0060182

MILLS, J.C.; STONE, N.L.; ERHARDT, J. & PITTMAN, R.N. (1998). Apoptotic Membrane Blebbing Is Regulated by Myosin Light Chain Phosphorylation. *J. Cell Biol*. 140, 627–636. https://doi.org/10.1083/jcb.140.3.627

MORENO-MANZANO, V.; RODRIGUEZ-JIMENEZ, F.J.; GARCIA-ROSELLO, M.; LAINEZ, S.; ERCEG, S.; CALVO, M.T.; RONAGHI, M.; LLORET, M.; PLANELLS-CASES, R.; SANCHEZ-PUELLES, J.M. & STOJKOVIC, M. (2009). Activated spinal cord ependymal stem cells rescue neurological function. *Stem Cells* 27, 733–743. https://doi.org/10.1002/stem.24

NAKAJIMA, H.; UCHIDA, K.; GUERRERO, A.R.; WATANABE, S.; SUGITA, D.; TAKEURA, N.; YOSHIDA, A.; LONG, G.; WRIGHT, K.T.; JOHNSON, W.E.B. & BABA, H. (2012). Transplantation of Mesenchymal Stem Cells Promotes an Alternative Pathway of Macrophage Activation and Functional Recovery after Spinal Cord Injury. *J. Neurotrauma* 29, 1614–1625. https://doi.org/10.1089/neu.2011.2109

NIMMERJAHN, A.; KIRCHHOFF, F. & HELMCHEN, F. (2005). Resting microglial cells are highly dynamic surveillants of brain parenchyma in vivo. *Science* 308, 1314–8. https://doi.org/10.1126/science.1110647

OUDEGA, M. (2012). Molecular and cellular mechanisms underlying the role of blood vessels in spinal cord injury and repair. *Cell Tissue Res*. 349, 269–288. https://doi.org/10.1007/s00441-012-1440-6

PASTERKAMP, R.J.; GIGER, R.J.; RUITENBERG, M.-J.; HOLTMAAT, A.J.G.D.; DE WIT, J.; DE WINTER, F. & VERHAAGEN, J. (1999). Expression of the Gene Encoding the Chemorepellent Semaphorin III Is Induced in the Fibroblast Component of Neural Scar Tissue Formed Following Injuries of Adult But Not Neonatal CNS. *Mol. Cell. Neurosci*. 13, 143–166. https://doi.org/10.1006/MCNE.1999.0738

PEARSE, D.D.; PEREIRA, F.C.; MARCILLO, A.E.; BATES, M.L.; BERROCAL, Y.A.; FILBIN, M.T. & BUNGE, M.B. (2004). cAMP and Schwann cells promote axonal growth and functional recovery after spinal cord injury. *Nat. Med*. 10, 610–616. https://doi.org/10.1038/nm1056

PERLSON, E.; HANZ, S.; BEN-YAAKOV, K.; SEGAL-RUDER, Y.; SEGER, R. & FAINZILBER, M. (2005). Vimentin-dependent spatial translocation of an activated MAP kinase in injured nerve. *Neuron* 45, 715–26. https://doi.org/10.1016/j.neuron.2005.01.023

PIAZZOLLA, D.; MEISSL, K.; KUCEROVA, L.; RUBIOLO, C. & BACCARINI, M. (2005). Raf-1 sets the threshold of Fas sensitivity by modulating Rok-α signaling. *J. Cell Biol*. 171, 1013–1022. https://doi.org/10.1083/jcb.200504137

PLEMEL, J.R.; KEOUGH, M.B.; DUNCAN, G.J.; SPARLING, J.S.; YONG, V.W.; STYS, P.K. & TETZLAFF, W. (2014). Remyelination after spinal cord injury: Is it a target for repair? *Prog. Neurobiol*. 117, 54–72. https://doi.org/10.1016/J.PNEUROBIO.2014.02.006

POPOVICH, P.G. & LONGBRAKE, E.E. (2008). Can the immune system be harnessed to repair the CNS? *Nat. Rev. Neurosci*. 9, 481–493. https://doi.org/10.1038/nrn2398

PUTTAGUNTA, R.; TEDESCHI, A.; SÓRIA, M.G.; HERVERA, A.; LINDNER, R.; RATHORE, K.I.; GAUB, P.; JOSHI, Y.; NGUYEN, T.; SCHMANDKE, A.; LASKOWSKI, C.J.; BOUTILLIER, A.-L.; BRADKE, F. & DI GIOVANNI, S. (2014). PCAF-dependent epigenetic changes promote axonal regeneration in the central nervous system. *Nat. Commun*. 5, 3527. https://doi.org/10.1038/ncomms4527

QUADRATO, G. & DI GIOVANNI, S. (2013). Waking up the sleepers: shared transcriptional pathways in axonal regeneration and neurogenesis. *Cell. Mol. Life Sci*. 70, 993–1007. https://doi.org/10.1007/s00018-012-1099-x

REIER, P.J. & HOULE, J.D. (1988). The glial scar: its bearing on axonal elongation and transplantation approaches to CNS repair. *Adv. Neurol*. 47, 87–138.

RENA, G.; HARDIE, D.G. & PEARSON, E.R. (2017). The mechanisms of action of metformin. *Diabetologia* 60, 1577–1585. https://doi.org/10.1007/s00125-017-4342-z

RICHARDSON, P.M.; MCGUINNESS, U.M. & AGUAYO, A.J. (1980). Axons from CNS neurones regenerate into PNS grafts. *Nature* 284, 264–265. https://doi.org/10.1038/284264a0

RODRÍGUEZ-JIMÉNEZ, F.J.; ALASTRUE-AGUDO, A.; ERCEG, S.; STOJKOVIC, M. & MORENO-MANZANO, V. (2012). FM19G11 Favors Spinal Cord Injury Regeneration and Stem Cell Self-Renewal by Mitochondrial Uncoupling and Glucose Metabolism Induction. *Stem Cells* 30, 2221–2233. https://doi.org/10.1002/stem.1189

ROMERO, M.I.; RANGAPPA, N.; GARRY, M.G. & SMITH, G.M. (2001). Functional regeneration of chronically injured sensory afferents into adult spinal cord after neurotrophin gene therapy. *J. Neurosci*. 21, 8408–16. https://doi.org/10.1523/JNEUROSCI.21-21-08408.2001

RUDGE, J.S. & SILVER, J. (1990). Inhibition of neurite outgrowth on astroglial scars in vitro. *J. Neurosci.* 10, 3594–603. https://doi.org/10.1523/JNEUROSCI.10-11-03594.1990

SCHWAIGER, F.-W.; SCHMITT, G.H.; ANDREAS B.; HORVAT, A.; HAGER, G.; STREIF, R.; SPITZER, C.; GAMAL, S.; BREUER, S.; BROOK, G.A.; NACIMIENTO, W. & KREUTZBERG, G.W. (2000). Peripheral but not central axotomy induces changes in Janus kinases (JAK) and signal transducers and activators of transcription (STAT). *Eur. J. Neurosci*. 12, 1165–1176. https://doi.org/10.1046/j.1460-9568.2000.00005.x

SEIJFFERS, R.; MILLS, C.D. & WOOLF, C.J. (2007). ATF3 Increases the Intrinsic Growth State of DRG Neurons to Enhance Peripheral Nerve Regeneration. *J. Neurosci*. 27, 7911–7920. https://doi.org/10.1523/JNEUROSCI.5313-06.2007

SEZER, N.; AKKUŞ, S. & UĞURLU, F.G. (2015). Chronic complications of spinal cord injury. *World J. Orthop*. 6, 24. https://doi.org/10.5312/wjo.v6.i1.24

SHEN, Y.; TENNEY, A.P.; BUSCH, S.A.; HORN, K.P.; CUASCUT, F.X.; LIU, K.; HE, Z.; SILVER, J. & FLANAGAN, J.G. (2009). PTPsigma is a receptor for chondroitin sulfate proteoglycan, an inhibitor of neural regeneration. *Science* 326, 592–6.

https://doi.org/10.1126/science.1178310

SHI, J. & WEI, L. (2007). Rho kinase in the regulation of cell death and survival. *Arch. Immunol. Ther. Exp*. (Warsz). 55, 61–75. https://doi.org/10.1007/s00005-007-0009-7

SHIBUYA, M.; HIRAI, S.; SETO, M.; SATOH, S. & OHTOMO, E. (2005). Fasudil Ischemic Stroke Study Group. Effects of fasudil in acute ischemic stroke: results of a prospective placebo-controlled double-blind trial. *J. Neurol. Sci*. 238, 31–9. https://doi.org/10.1016/j.jns.2005.06.003

SHIHABUDDIN, L.S.; RAY, J. & GAGE, F.H. (1997). FGF-2 Is Sufficient to Isolate Progenitors Found in the Adult Mammalian Spinal Cord. *Exp. Neurol.* 148, 577–586. https://doi.org/10.1006/EXNR.1997.6697

SOFRONIEW, M. V. (2018). Dissecting spinal cord regeneration perspective. *Nature* 557, 343–350. https://doi.org/10.1038/s41586-018-0068-4

SOFRONIEW, M. V. (2014). Astrogliosis. Cold Spring Harb. *Perspect. Biol.* 7, a020420. https://doi.org/10.1101/cshperspect.a020420

STARKEY, M.L.; BARTUS, K.; BARRITT, A.W. & BRADBURY, E.J. (2012). Chondroitinase ABC promotes compensatory sprouting of the intact corticospinal tract and recovery of forelimb function following unilateral pyramidotomy in adult mice. *Eur. J. Neurosci.* 36, 3665–3678. https://doi.org/10.1111/ejn.12017

SUN, F.; PARK, K.K.; BELIN, S.; WANG, D.; LU, T.; CHEN, G.; ZHANG, K.; YEUNG, C.; FENG, G.; YANKNER, B.A. & HE, Z. (2011). Sustained axon regeneration induced by co-deletion of PTEN and SOCS3. *Nature* 480, 372–375. https://doi.org/10.1038/nature10594

TAKEOKA, A.; JINDRICH, D.L.; MUÑOZ-QUILES, C.; ZHONG, H.; VAN DEN BRAND, R.; PHAM, D.L.; ZIEGLER, M.D.; RAMÓN-CUETO, A.; ROY, R.R.; EDGERTON, V.R. & PHELPS, P.E. (2011). Axon regeneration can facilitate or suppress hindlimb function after olfactory ensheathing glia transplantation. *J. Neurosci*. 31, 4298–310. https://doi.org/10.1523/JNEUROSCI.4967-10.2011

TAN, H.-B.; ZHONG, Y.-S.; CHENG, Y. & SHEN, X. (2011). Rho/ROCK pathway and neural regeneration: a potential therapeutic target for central nervous system and optic nerve damage. *Int. J. Ophthalmol*. 4, 652–7. https://doi.org/10.3980/j.issn.2222-3959.2011.06.16

TOTOIU, M.O. & KEIRSTEAD, H.S. (2005). Spinal cord injury is accompanied by chronic progressive demyelination. *J. Comp. Neurol.* 486, 373–383. https://doi.org/10.1002/cne.20517

TRAN, A.P.; WARREN, P.M. & SILVER, J. (2018). The Biology of Regeneration Failure and Success After Spinal Cord Injury. *Physiol. Rev.* 98, 881–917. https://doi.org/10.1152/physrev.00017.2017

TUSZYNSKI, M.H.; PETERSON, D.A.; RAY, J.; BAIRD, A.; NAKAHARA, Y.& GAGES, F.H. (1994). Fibroblasts Genetically Modified to Produce Nerve Growth Factor Induce Robust Neuritic Ingrowth after Grafting to the Spinal Cord. *Exp. Neurol*. 126, 1–14. https://doi.org/10.1006/EXNR.1994.1037

TUSZYNSKI, M.H. & STEWARD, O. (2012). Concepts and methods for the study of axonal regeneration in the CNS. *Neuron* 74, 777–91. https://doi.org/10.1016/j.neuron.2012.05.006

VAARMANN, A.; MANDEL, M.; ZEB, A.; WARESKI, P.; LIIV, J.; KUUM, M.; ANTSOV, E.; LIIV, M.; CAGALINEC, M.; CHOUBEY, V. & KAASIK, A. (2016). Mitochondrial biogenesis is required for axonal growth. *Development* 143, 1981–92. https://doi.org/10.1242/dev.128926

VAN DEN BRAND, R.; HEUTSCHI, J.; BARRAUD, Q.; DIGIOVANNA, J.; BARTHOLDI, K.; HUERLIMANN, M.; FRIEDLI, L.; VOLLENWEIDER, I.; MORAUD, E.M.; DUIS, S.; DOMINICI, N.; MICERA, S.; MUSIENKO, P. & COURTINE, G. (2012). Restoring voluntary control of locomotion after paralyzing spinal cord injury. *Science* (80). 336, 1182–1185. https://doi.org/10.1126/science.1217416

VAN NIEKERK, E.A.; TUSZYNSKI, M.H.; LU, P. & DULIN, J.N. (2016). Molecular and Cellular Mechanisms of Axonal Regeneration After Spinal Cord Injury. *Mol. Cell. Proteomics* 15, 394–408. https://doi.org/10.1074/mcp.r115.053751

VERMA, P.; CHIERZI, S.; CODD, A.M.; CAMPBELL, D.S.; MEYER, R.L.; HOLT, C.E. & FAWCETT, J.W. (2005). Axonal protein synthesis and degradation are necessary for efficient growth cone regeneration. *J. Neurosci*. 25, 331–42. https://doi.org/10.1523/JNEUROSCI.3073-04.2005

VOGELAAR, C.F.; KÖNIG, B.; KRAFFT, S.; ESTRADA, V.; BRAZDA, N.; ZIEGLER, B.; FAISSNER, A. & MÜLLER, H.W. (2015). Pharmacological Suppression of CNS Scarring by Deferoxamine Reduces Lesion Volume and Increases Regeneration in an In Vitro Model for Astroglial-Fibrotic Scarring and in Rat Spinal Cord Injury In Vivo. *PLoS One 10*, e0134371. https://doi.org/10.1371/journal.pone.0134371

WAGNER, F.B.; MIGNARDOT, J.B.; LE GOFF-MIGNARDOT; C.G.; DEMESMAEKER, R.; KOMI, S.; CAPOGROSSO, M.; ROWALD, A., SEÁÑEZ, I.; CABAN, M.; PIRONDINI, E.; VAT, M.; MCCRACKEN, L.A.; HEIMGARTNER, R.; FODOR, I.; WATRIN, A.; SEGUIN, P.; PAOLES, E.; VAN DEN KEYBUS, K.; EBERLE, G.; SCHURCH, B.; PRALONG, E.; BECCE, F.; PRIOR, J.; BUSE, N.; BUSCHMAN, R.; NEUFELD, E.; KUSTER, N.; CARDA, S.; VON ZITZEWITZ, J.; DELATTRE, V.; DENISON, T.; LAMBERT, H.; MINASSIAN, K.; BLOCH, J. & COURTINE, G. (2018). Targeted neurotechnology restores walking in humans with spinal cord injury. *Nature* 563, 65–93. https://doi.org/10.1038/s41586-018-0649-2

WANG, B.; IYENGAR, R.; LI-HARMS, X.; JOO, J.H.; WRIGHT, C.; LAVADO, A.; HORNER, L.; YANG, M.; GUAN, J.-L.; FRASE, S.; GREEN, D.R.; CAO, X. & KUNDU, M. (2018). The autophagy-inducing kinases, ULK1 and ULK2, regulate axon guidance in the developing mouse forebrain via a noncanonical pathway. *Autophagy* 14, 796–811. https://doi.org/10.1080/15548627.2017.1386820

WANNER, I.B.; ANDERSON, M.A.; SONG, B.; LEVINE, J.; FERNANDEZ, A.; GRAY-THOMPSON, Z.; AO, Y. & SOFRONIEW, M. V. (2013). Glial Scar

Borders Are Formed by Newly Proliferated, Elongated Astrocytes That Interact to Corral Inflammatory and Fibrotic Cells via STAT3-Dependent Mechanisms after Spinal Cord Injury. *J. Neurosci*. 33, 12870–12886. https://doi.org/10.1523/JNEUROSCI.2121-13.2013

WEISS, S.; DUNNE, C.; HEWSON, J.; WOHL, C.; WHEATLEY, M.; PETERSON, A.C. & REYNOLDS, B.A. (1996). Multipotent CNS stem cells are present in the adult mammalian spinal cord and ventricular neuroaxis. *J. Neurosci.* 16, 7599–609. https://doi.org/10.1523/JNEUROSCI.16-23-07599.1996

WILLIAMS, R.R.; HENAO, M.; PEARSE, D.D. & BUNGE, M.B. (2015). Permissive Schwann Cell Graft/Spinal Cord Interfaces for Axon Regeneration. *Cell Transplant*. 24, 115–131. https://doi.org/10.3727/096368913X674657

WILLIAMS, T.; COURCHET, J.; VIOLLET, B.; BRENMAN & J.E. POLLEUX, F. (2011). AMP-activated protein kinase (AMPK) activity is not required for neuronal development but regulates axogenesis during metabolic stress. *Proc. Natl. Acad. Sci. U. S. A*. 108, 5849–54. https://doi.org/10.1073/pnas.1013660108

WORLD HEALTH ORGANIZATION (2013, November 19). Spinal Cord Injury. Retrieved the 17TH June 2019 from: https://www.who.int/en/news-room/fact-sheets/detail/spinal-cord-injury.

WU, J.; LI, J.; HU, H.; LIU, P.; FANG, Y. & WU, D. (2012). Rho-kinase inhibitor, fasudil, prevents neuronal apoptosis via the akt activation and pten inactivation in the ischemic penumbra of rat brain. *Cell. Mol. Neurobiol*. 32, 1187–1197. https://doi.org/10.1007/s10571-012-9845-z

WU, X. & XU, X. (2016). RhoA / Rho kinase in spinal cord injury. *Neural Regeneration Research* 11 (1), 23–27. https://doi.org/10.4103/1673-5374.169601

YAMAGUCHI, H.; KASA, M.; AMANO, M.; KAIBUCHI, K. & HAKOSHIMA, T. (2006). Molecular mechanism for the regulation of rho-kinase by dimerization and its inhibition by fasudil. *Structure* 14, 589–600. https://doi.org/10.1016/j.str.2005.11.024

YANG, X.; LIU, Y.; LIU, C.; XIE, W.; HUANG, E.; HUANG, W.; WANG, J.; CHEN, L.; WANG, HUIPIN, QIU, P.; XU, J.; ZHANG, F.; WANG & HUIJUN (2013). Inhibition of ROCK2 expression protects against methamphetamine-induced neurotoxicity in PC12 cells. *Brain Res. 1533*, 16–25. https://doi.org/10.1016/J.BRAINRES.2013.08.009

YOKOTA, K.; KUBOTA, K.; KOBAYAKAWA, K.; SAITO, T.; HARA, M.; KIJIMA, K.; MAEDA, T.; KATOH, H.; OHKAWA, Y.; NAKASHIMA, Y. & OKADA, S. (2019). Pathological changes of distal motor neurons after complete spinal cord injury. *Mol. Brain* 12, 4. https://doi.org/10.1186/s13041-018-0422-3

YOO, S.; KIM, H.H.; KIM, P.; DONNELLY, C.J.; KALINSKI, A.L.; VUPPALANCHI, D.; PARK, M.; LEE, S.J.; MERIANDA, T.T.; PERRONE-BIZZOZERO, N.I. & TWISS, J.L. (2013). A HuD-ZBP1 ribonucleoprotein complex localizes GAP-43 mRNA into axons through its 3' untranslated region AU-rich regulatory element. *J. Neurochem*. 126, 792–804. https://doi.org/10.1111/jnc.12266

ZHOU, L.; BAUMGARTNER, B.J.; HILL-FELBERG, S.J.; MCGOWEN, L.R.; SHINE, H.D.; HARVEY, A.; BENOWITZ, L.; EDGERTON, V. & TUSZYNSKI, M. (2003). Neurotrophin-3 expressed in situ induces axonal plasticity in the adult injured spinal cord. *J. Neurosci*. 23, 1424–31. https://doi.org/10.1523/jneurosci.4070-05.2005

ZUKOR, K.; BELIN, S.; WANG, C.; KEELAN, N.; WANG, X. & HE, Z. (2013). Short hairpin RNA against PTEN enhances regenerative growth of corticospinal tract axons after spinal cord injury. *J. Neurosci*. 33, 15350–61. https://doi.org/10.1523/JNEUROSCI.2510-13.2013

VII. ANNEX

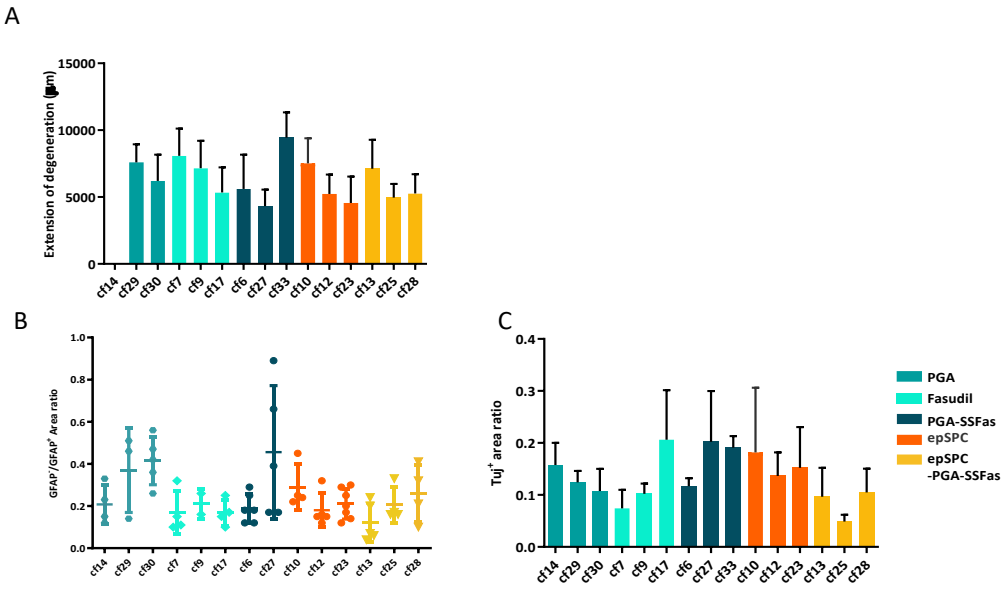

Supplementary figure 1.Data per animals. (A) Mean values of the extension of degeneration per animal. **(B)**GFAP⁻/GFAP⁺ area ratio per animal and **(B)** Tuj⁺ area ratio per animal.

Supplementary table 1. Data for binomial proportion significance statistical analysis of GAP43⁺ proportions.

Treatment	Control	Met	CC	CC-FL50	CC-FL100	CC-SS50	CC-SS100	LPA	LPA-Met
Proportion	0,269	0,280	0,209	0,476	0,467	0,524	0,664	0.328	0.373
N GAP43⁺	220	273	299	280	276	160	190	220	257
N total	816	973	1429	588	590	305	286	671	688
significance against control	-	ns	*	***	***	***	***	ns	***
p-value α=0.01	-	0,61	1,10E-3	1,55E-15	1,67E-14	8,88E-16	0,00E+00	1.43E-02	1.6E-05
Significance against Met or LPA-Met	-	-	***	****	****	****	****	-	-
p-value α=0.01			5,59E-05	4,88E-15	5,68E-14	4,00E-15	0,00E+00		
Treatment	**LPA-CC**	**LPA-FL50**	**LPA-FL100**	**LPA-SS50**	**LPA-SS100**	**LPA-CC-FL50**	**LPA-CC-FL100**	**LPA-CC-SS50**	**LPA-CC-SS100**
Proportion	0,335	0,359	0,354	0,504	0,404	0,347	0,455	0,552	0,364
N GAP43⁺	178	165	274	362	247	219	233	227	277
N total	532	460	773	718	611	632	512	411	760
significance against control	-	**	**	****	****	*	****	****	***
p-value α=0.01	1,06E-02	8,72E-04	2,60E-04	0,00E+00	8,16E-08	1,59E-03	3,97E-12	0,00E+00	5,1E-05
Significance against Met or LPA-Met	ns	ns	****	ns	*	****	ns	ns	ns
p-value α=0.01	1,63E-01	4,38E-01	8,41E-07	3,16E-01	4.5E-03	8,13E-09	7,21E-01	1,63E-01	6,16E-01

Supplementary table 2. Data for binomial proportion significance statistical analysis of Casp 3⁺ proportions.

Treatment	Control	CC	CC-NAC	Fas50	Fas100	SSFas-50	SSFas-100	CC-Fas50	CC-Fas100	CC-SSFas50	CC-SSFas100
Proportion	0,072	0,3225	0,1324	0,1485	0,1405	0,0438	0,1728	0,3317	0,3789	0,1578	0,2088
N Casp3⁻	125	186	317	249	185	251	214	214	304	171	158
N Casp3⁺	9	60	42	37	26	11	37	71	115	27	33
TOTAL	134	246	359	286	211	262	251	285	419	198	191
significance against control	-	****	ns	*	ns	ns	**	****	****	*	***
p-value α=0.05	-	3,58E-08	0,0621	0,026	0,0508	0,23775	0,00621	1,15E-08	2,04E-11	0,019493	0,000728
significance against CC	-	-	-	****	****	****	***	ns	ns	****	**
p-value α=0.05	-	-	-	1.9E-06	5.3E-06	2.2E-16	1.1E-04	0,82177	0,147892	6,66E-05	0,008115